BUILDING SIMPLIFIED MODEL VALIDATION

5.1. Introduction

Lumped building models have already been developed by Laret [18], Ngendakumana [22], Kummert [17], Wang [13]. Our purpose is to validate such models by comparing their results to those provided by a detailed dynamic model. The validation process can lead either to add more parameters to the model in order to improve its reliability, or to suppress some parameters in order to simplify the model while keeping good quality results, in agreement with the model simulation objectives.

The results of the *simplified dynamic model* proposed in §4.3 and 4.4 can be compared to those provided by a *reference* convolution model based on response factors [24], [25]. Three error indicators can be used to compare the indoor temperature profiles generated by both models (§5.3.2). The dampening factors can also be computed by comparison with a simple static model.

A one zone simplified model such as that presented on fig 4.2 can be generated from the exact detailed description of the walls compositions. It can be validated for five two levels houses and for an office room (§5.4).

A one zone simplified model can also be generated from wall *default parameters* resulting from the typology established in chapter 3 §5. It can also be validated for five houses and for an office room, allowing a much easier way to introduce wall dynamic data for the model user (§5.4).

A wall model can be adopted for partition walls, so that a two zones simplified model can be generated. That model can be validated for two houses, one including massive partition walls, the other one including light partition walls (§5.5).

The *simplified dynamic model* must be able to estimate summer overheating risks with enough accuracy. So, a specific 2R1C branch can be added to account for roof absorbed solar heat gains and for sky infrared radiation. That model can be validated by comparison with a reference convolution model including all the opaque building walls absorbed solar gains and sky infrared radiation (§5.6).

The one zone *simplified dynamic model* can be tested on the experimental results provided by EMPA test cell in the framework of IEA-ECBCS annex 43 research project. The results are presented in § 5.8.

5.2. Reference model

The reference model can be provided by a response factors convolution process.

5.2.1. Walls response factors

Response factors can be computed for each wall:

- For isothermal boundary conditions walls, a triangular temperature impulse with a maximum 1 *K* value is imposed on the indoor side, while the outdoor side temperature is maintained at a null value. The response factors of indoor heat flow *Z* and outdoor heat flow *Y* are computed (fig.5.1). *Y* outdoor heat flows are small but they can bring a significant contribution for when exposed is summer roofs.

- For adiabatic boundary conditions walls, a similar triangular temperature impulse is imposed on the indoor side while the outdoor side heat flow is null. The response factor of indoor heat flow *Z* is computed (fig.5.2).

The triangular temperature impulse basis equals $2.\Delta t$, where Δt is the computation time step.

Heat response factors can be computed with EES solver, using a finite elements method with a Crank Nicholson time integration process:

$$\mathbf{C}.\left(\boldsymbol{\theta}_{t+\Delta t} - \boldsymbol{\theta}_t\right) + \left(\mathbf{L} + \mathbf{H}\right).\frac{\Delta t}{2}.\left(\boldsymbol{\theta}_{t+\Delta t} + \boldsymbol{\theta}_t\right) = \Delta t.\mathbf{H}.\left(\boldsymbol{\theta}_{e,t+\Delta t} + \boldsymbol{\theta}_{e,t}\right) \qquad (5.1)$$

C: Capacity matrix *J/K* $\qquad\qquad \mathbf{C} = \int_V \mathbf{N}^T.\rho.c.\mathbf{N}.dV$

L: Conductivity matrix *W/K* $\qquad\qquad \mathbf{L} = \int_V \mathbf{B}^T.\lambda.\mathbf{B}.dV$

H: Convection and radiation matrix *W/K* $\qquad \mathbf{H} = \int_{S_e} h.\mathbf{N}_S^T.\mathbf{N}_S.dS$

N	: Element temperature interpolation matrix	-
B	: Element temperature-gradient interpolation matrix	m^{-1}
$\mathbf{N}_S$	: Elements surface temperature interpolation matrix	-

h : Heat transfer coefficient, including convection and radiation effects $W/m^2.K$
Δt : Computation time step *s*
$\boldsymbol{\theta}_t, \boldsymbol{\theta}_{t+\Delta t}$: Vectors of nodal temperatures $°C$, at time *t* and at time $t+\Delta t$
$\boldsymbol{\theta}_{e,t}, \boldsymbol{\theta}_{e,t+\Delta t}$: Vectors of environmental temperatures on surface S_e at time *t*, and at time $t+\Delta t$

The heat transfer coefficient *h* is supposed to be independent from temperature.

The wall is decomposed into 14 finite elements of degree 2 through parabolic interpolation functions. Wall response factors are computed with EES solver with a time step of 600 s during 100 h. They are used as input of a convolution process performed with a 1200 s time step.
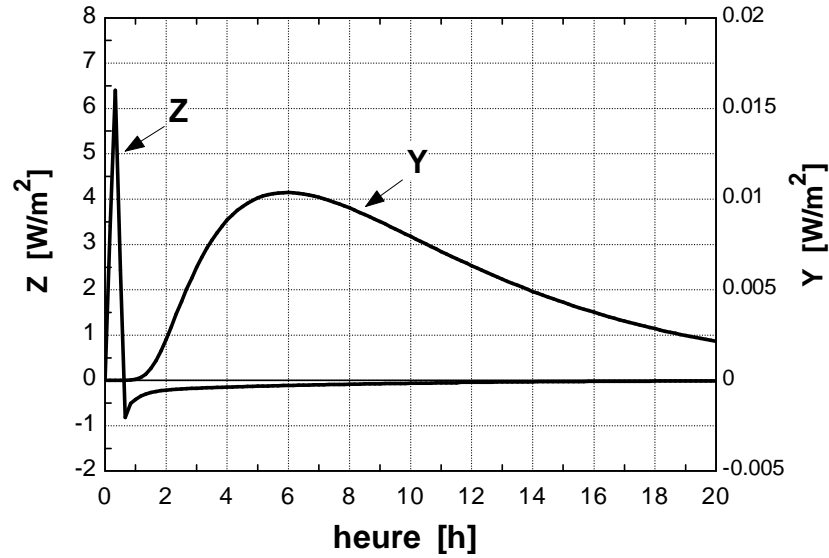
Fig.5.1. Response factors to a triangular indoor temperature impulse, computed for an isothermal boundary conditions wall.
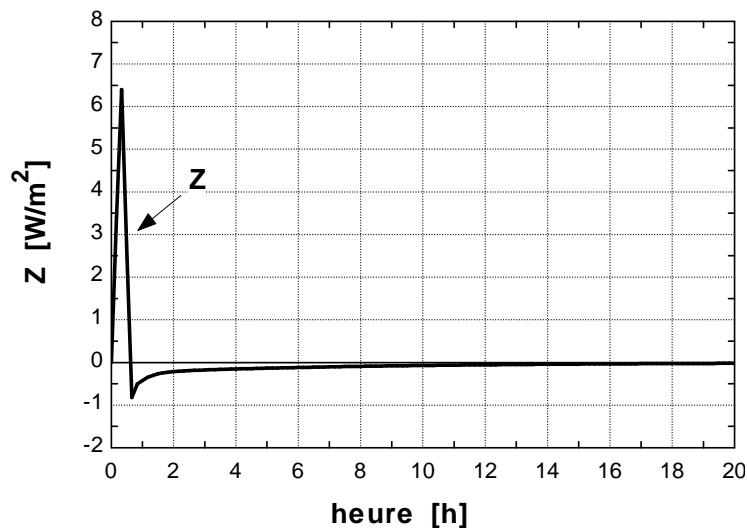

Fig.5.2. Response factors to a triangular indoor temperature impulse, computed for an adiabatic boundary conditions wall.

5.2.2. Convolution process

The wall response factors can be combined with each other to get the response factors corresponding to the whole building zone under study. A convolution process is then applied in order to provide the temperature and heat flow response of the building when it is submitted to a varying outdoor temperature and to a varying indoor set point temperature. The indoor heat flow resulting from the convolution is given by:

$$\dot{Q}_{convol} = \dot{Q}_{out,isothermal} - \dot{Q}_{in,isothermal} - \dot{Q}_{in,adiabatic} \qquad (5.2)$$

$$\dot{Q}_{out,isothermal} = \sum_{i=1}^{n-1} Y_{i.\Delta t} . t_{out,t-(i-1).\Delta t} + Y_{n\Delta t} . \sum_{j=1}^{j\,max} \lambda_{out,isothermal}^{j} . t_{out,t-(n+j)\Delta t}$$

$$\dot{Q}_{in,isothermal} = \sum_{i=1}^{n-1} Z_{i.\Delta t} . t_{in,t-(i-1).\Delta t} + Z_{n\Delta t} . \sum_{j=1}^{j\,max} \lambda_{in,isothermal}^{j} . t_{in,t-(n+j)\Delta t} \qquad (5.3)$$

$$\dot{Q}_{in,adiabatic} = \sum_{i=1}^{n-1} Z_{i.\Delta t} . t_{in,t-(i-1).\Delta t} + Z_{n\Delta t} . \sum_{j=1}^{j\,max} \lambda_{adiabatic}^{j} . t_{in,t-(n+j)\Delta t}$$

$\dot{Q}_{out,isothermal}$: Indoor heat flow response to outdoor temperature W

$\dot{Q}_{in,isothermal}$: Indoor heat flow response to indoor temperature for isothermal boundary conditions walls W

$\dot{Q}_{in,adiabatic}$: Indoor heat flow response to indoor temperature for adiabatic boundary conditions walls W

$$j_{max} = \frac{t}{\Delta t} - n$$

n : Number of time steps covered by the response curve

t : Time since the beginning of the computation s

Δt : Computation time step s

When the time t is varying from 0 to infinity, the integration of the whole response curve Y or Z must equal the building heat loss coefficient AU. As the computed response curve is described by a limited number of terms n, it is shortened. A correction is then needed in order to reproduce the steady state behavior of the building. The second term of each equation (5.3) is intended to perform this correction, with:

$$\lambda_{out,isothermal} = \frac{AU - \sum_{i=1}^{n} . Y_{i\Delta t}}{AU - \sum_{i=1}^{n} . Y_{i\Delta t} + Y_{n\Delta t}} \qquad \lambda_{in,isothermal} = \frac{AU - \sum_{i=1}^{n} . Z_{i\Delta t}}{AU - \sum_{i=1}^{n} . Z_{i\Delta t} + Z_{n\Delta t}} \qquad (5.4)$$

$$\lambda_{in,adiabatic} = \frac{- \sum_{i=1}^{n} . Z_{i\Delta t}}{- \sum_{i=1}^{n} . Z_{i\Delta t} + Z_{n\Delta t}}$$

The building heat balance is given by the following equations, which can be compared to the simplified model equations (4.1),(4.2),(4.3):

$$dU_{c4,li}\backslash d\tau = \dot{Q}_{14,conv\,ol} + \dot{Q}_{14,vent,li} + \dot{Q}_{14,transm,li} + \dot{Q}_{4,li} \qquad (5.5)$$

$$\dot{Q}_{14,vent,li} = \frac{t_{1,li} - t_{4,li}}{R_5}$$

$$\dot{Q}_{14,transm,li} = \frac{t_{1,li} - t_{4,li}}{R_1}$$

$$\dot{Q}_{4,li} = \dot{Q}_{heating,li} + \dot{Q}_{sol,gl} + \dot{Q}_{occ}$$

$$U_{c4,li} = U_{c4,li,init} + \int_{\tau_{initial}}^{\tau_{final}} (dU_{c4,li\backslash dtau})\ d\tau$$

$$t_{4,li} = \frac{U_{c4,li}}{C_4}$$

5.1.3. Definition of a control law

The building heat balance, described by the simplified model equations (4.1) to (4.3), or computed by a convolution process according to equations (5.2) to (5.5), still presents one degree of freedom. It is necessary to introduce a relationship between the indoor temperature and the heating power supplied to the building zone. That is the control law, so that the heating power is governed by the difference between the indoor temperature and its set point, and limited by a maximum heating power (fig.5.3):

$$X = \mathbf{Min}\,(\,1\,,\ \mathbf{Max}\,(\,0\,,\ C \cdot (\,t_{set} - t_{in}\,)\,)\,)$$

(5.6)

$$\dot{Q}_{heating} = X \cdot \dot{Q}_{heating,max}$$
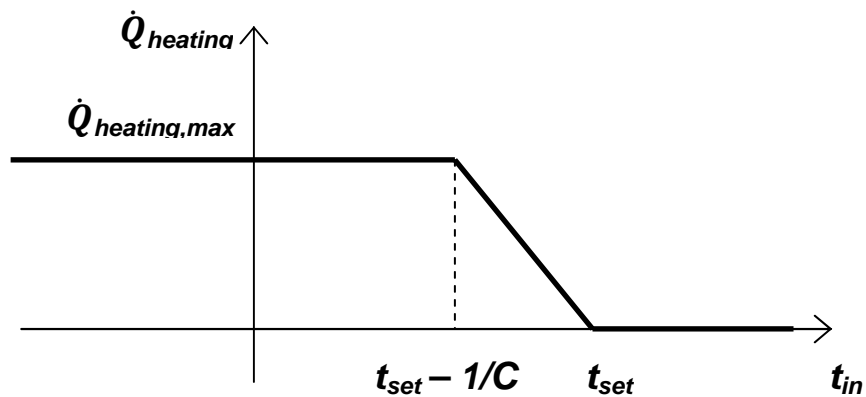
Fig 5.3: Feedback proportional control law.

5.3. Methodology

The results provided by the *simplified model* can be compared to those obtained through a *reference* convolution model based on response factors (§5.1), on a whole year simulation, for the five houses and the office room presented in chapter 4.
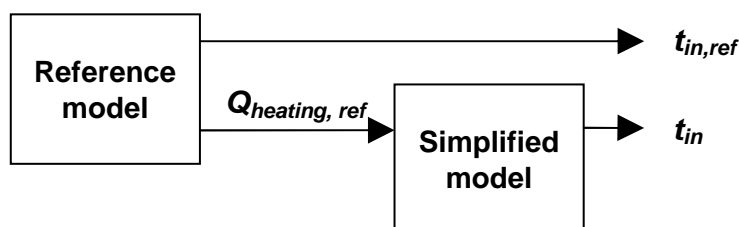

Fig.5.4. Simplified model validation.

A first computation on the reference model can yield a reference heat flow profile as well as an associated *reference indoor temperature profile*. Reference heat flows can be used as input data for the simplified model that generates an indoor temperature profile, t_{in}, which can be compared to the reference profile $t_{in,ref}$.

5.3.1 Occupancy profiles

Three occupancy profiles can be considered to validate the model:

- A *floating temperature* profile, i.e. there is no heating system, only solar and occupancy heat gains are considered, with constant occupancy heat gains,
- A *tertiary occupancy* profile, with a night set back and a stop during the week-end,
- A *residential occupancy* profile, starting in the morning from 6 to 8 AM, and restarting at the end of the afternoon until 11 PM, for each ordinary day. Heating is continuous during the week-end with a night set back.

A maximum value of occupancy heat gains is computed from a standard value of 5.42 *W/m²* *of floor area,* and weighted following a tertiary or residential occupancy profile (fig. 5.5).

Tertiary set point profile

Residential set point profile

Tertiary occupancy profile

Residential occupancy profile
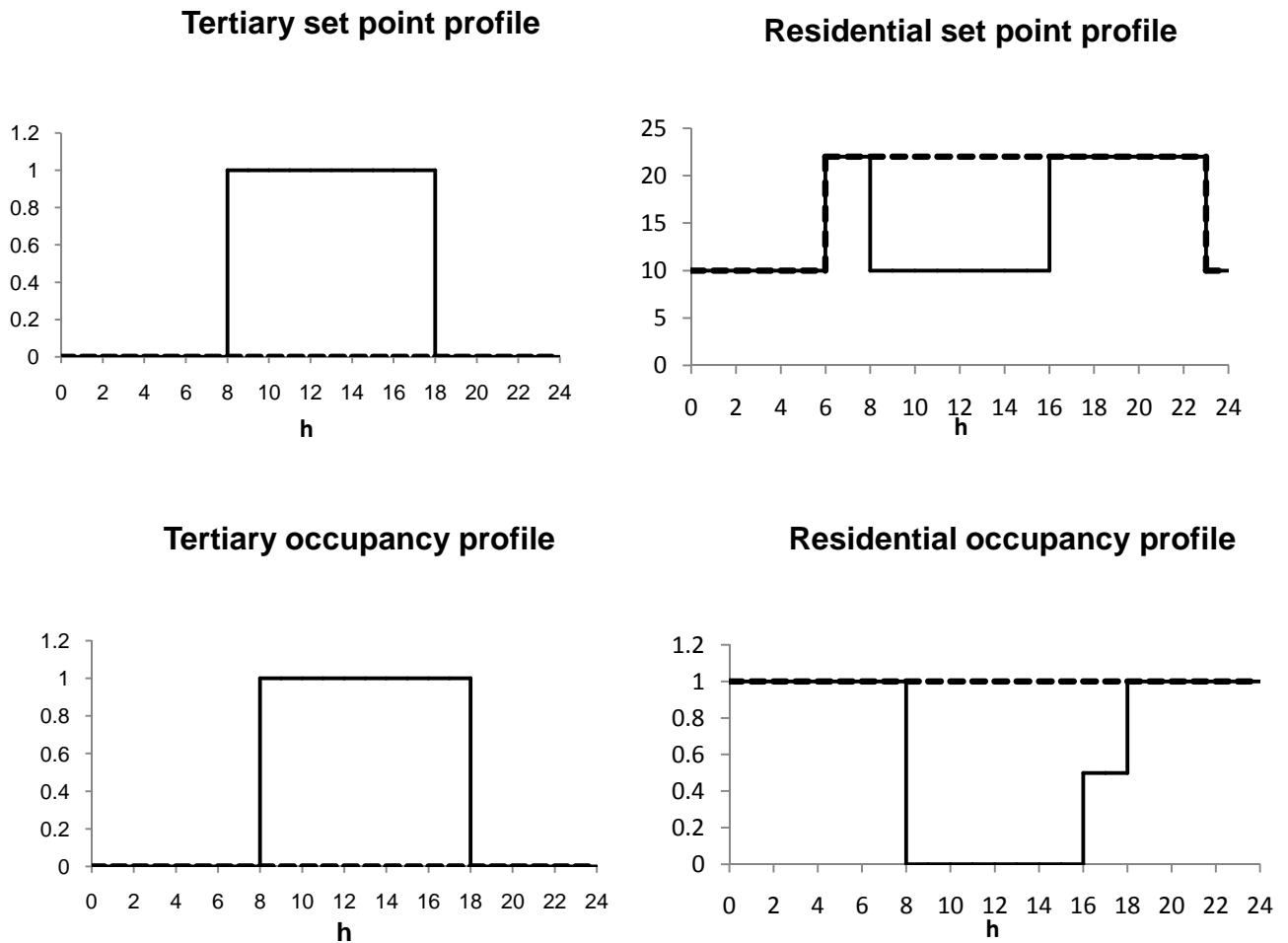
Fig.5.5. Temperature set points and occupancy heat gains factors for a tertiary profile (left) and a residential profile (right): full lines are related to ordinary days profiles while doted lines concerns the week-end profiles.

Fig. 5.6 shows the indoor temperature profiles in summer, and the same results in winter, with the corresponding heating powers, for Esneux house presented in chapter 4, modelled as a single zone. The weather data are reference weather data recorded in Uccle, Belgium.The occupancy pattern is a residential one. Dotted lines correspond to the detailed model results while continuous lines are related to the simplified model simulation. The two models are in agreement with each other.

Fig. 5.7 shows the same results in winter, for the office room presented in chapter 4, modelled as a single zone. The weather data are reference weather data recorded in Uccle, Belgium. The occupancy pattern is a tertiary one. The results are, again, close to each other, either for the office without suspended ceiling, or with suspended ceiling.
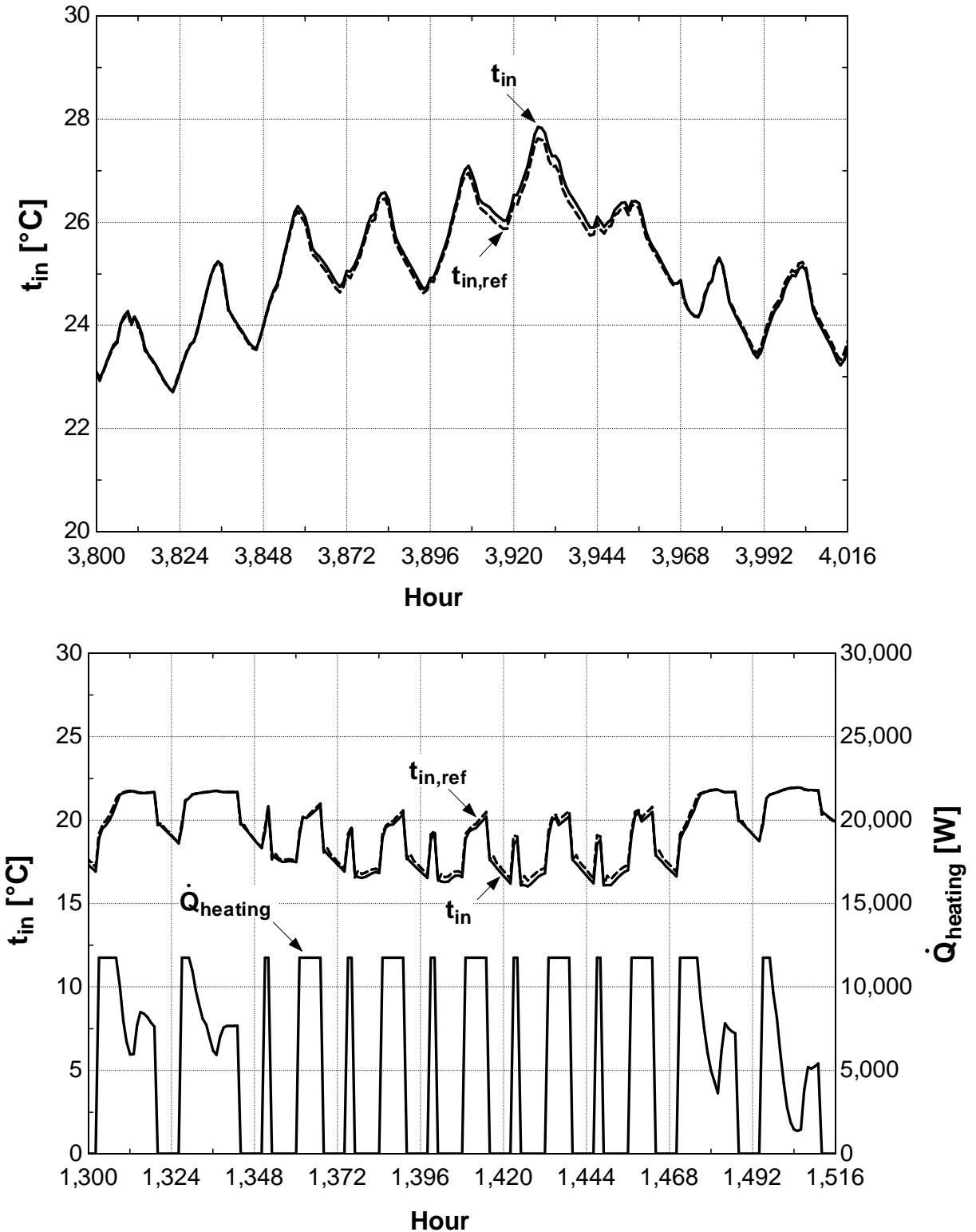
Fig. 5.6 Results provided by a zone simplified dynamic model, and by convolution process on response factors, for Esneux house in summer (up) and in winter (down). The occupancy profile is 'residential' (fig. 5.5).
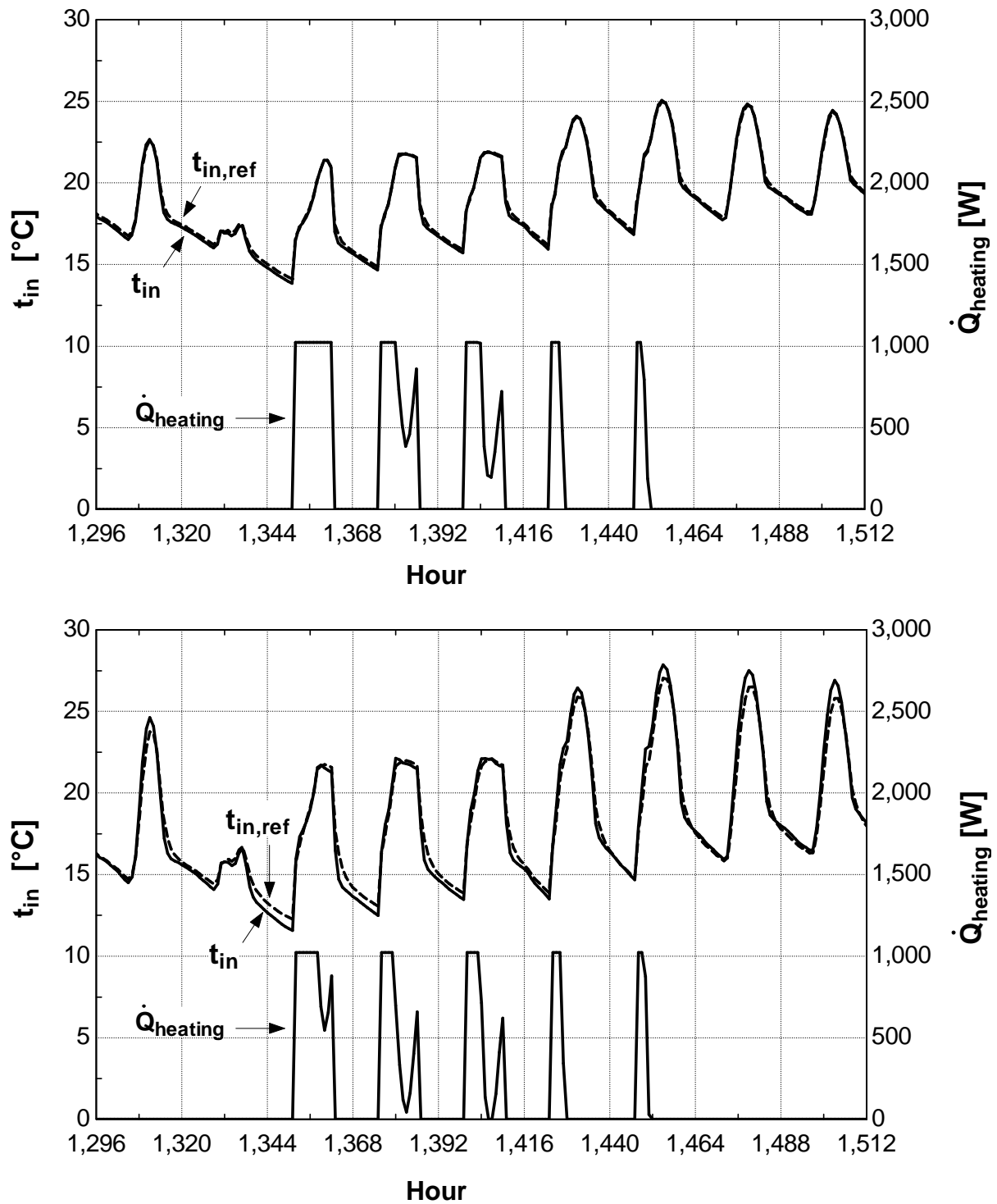
Fig. 5.7 Results provided by a zone simplified dynamic model, and by a convolution process on response factors, for the office room in winter without suspended ceiling (up) and with suspended ceiling (down). The occupancy profile is 'tertiary' (fig. 5.5).

5.3.2. Error indicators

Three indicators can be used to compare the reference and the simplified model indoor temperature profiles:

$$\bar{t}_{in} = \frac{\int\limits_{0}^{24h} t_{in}.d\tau}{24h} \qquad \Delta t_{in} = \sqrt{2\frac{\int\limits_{0}^{24h}(t_{in}-\bar{t}_{in})^2.d\tau}{24h}} \qquad RMS = \sqrt{\frac{\int\limits_{0}^{365j}(t_{in,ref}-t_{in})^2\,d\tau}{365j}} \qquad (5.7)$$

The first indicator gives the mean indoor temperature related to the last 24 h. It can be computed for the reference indoor temperature as well as for the indoor temperature profile to be validated. The differences $(\bar{t}_{in}-\bar{t}_{in,ref})$ can be calculated over the whole year.

The second indicator gives the mean indoor temperature amplitude related to the last 24 h, computed from the root-mean-square value of $(t_{in}-\bar{t}_{in})$. The differences $(\Delta t_{in}-\Delta t_{in,ref})$ can be calculated over the whole year.

The mean value μ and the standard deviation σ of the differences can be computed for both indicators, giving a confidence interval at 95 % limited by:

$$L_{95} = \mu \pm 1,96.\sigma$$

The third indicator is the root-mean-square value of the difference between the reference indoor temperature and the validated indoor temperature profile, computed over the whole year.

The simplified model can be considered as reliable if those three indicators are comprised between *-1 K* and *+1K*.

The first error indicator, corresponding to the mean indoor temperature, is very sensitive to the variations of the daily mean indoor temperature, particularly in the transient regime occurring at the beginning of the simulation. Fig. 5.8 displays the evolution of the error on the daily mean indoor temperature for Gesves house and for the office with ceiling, showing a higher error at the beginning of the simulation. So the first 1000 hours were omitted for the computation of the three error indicators, in order to reach a stationary state.

'Definition and Validation of a Simplified Multizone Dynamic Building Model Connected to Heating System and HVAC Unit'

*Heating System and HVAC Unit'*   *G. Masy*
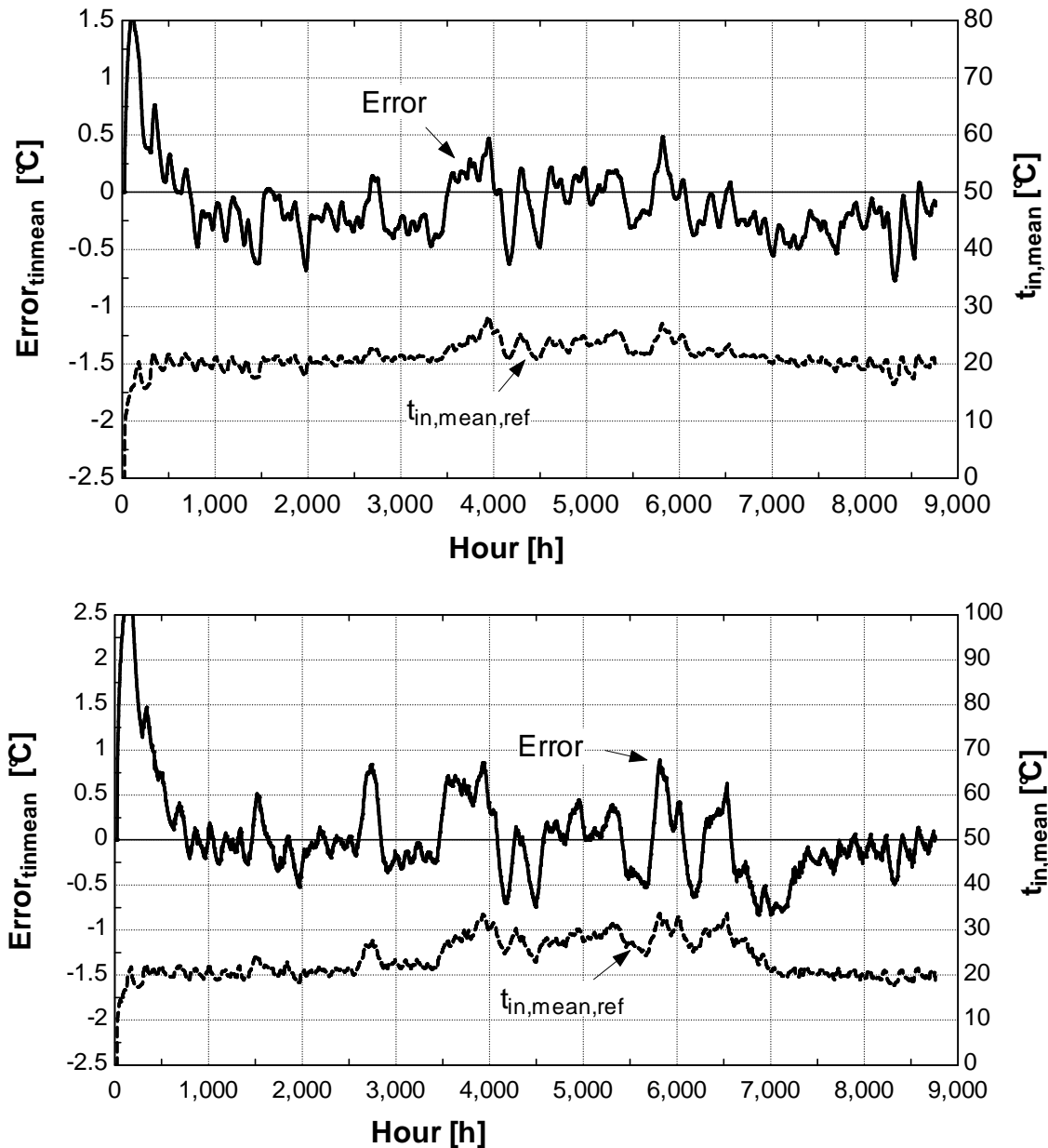
Fig. 5.8: Evolution of the error on the daily mean indoor temperature for Gesves house (up) and for the office room with suspended ceiling (down) - residential occupancy, walls exact θ φ parameters – Belgium reference weather data.

5.3.3. Dampening ratio

Apart from those three indicators meant to validate the simplified model, a fourth indicator can be related to the building dynamic. That is the yearly mean amplitude ratio $\overline{dmp}$ accounting for the indoor temperature dampening, compared to a static computation (static means that only model resistances are considered, and capacities are removed). The amplitude ratio can be computed for the reference indoor temperature profile and for the validated indoor temperature profile.

$$\overline{dmp} = \frac{\int_0^{365\,j} dmp.d\tau}{365\,j} \qquad \text{Where} \qquad dmp = 1 - \frac{\Delta t_{in}}{\Delta t_{in,st}}$$

With:

$$\Delta t_{in} = \sqrt{2\frac{\int_0^{24h}\left(t_{in} - \bar{t}_{in}\right)^2.d\tau}{24h}} \qquad \Delta t_{in,st} = \sqrt{2\frac{\int_0^{24h}\left(t_{in,st} - \bar{t}_{in,st}\right)^2.d\tau}{24h}} \qquad (5.8)$$

And:

$$\bar{t}_{in} = \frac{\int_0^{24h} t_{in}.d\tau}{24h} \qquad \bar{t}_{in,st} = \frac{\int_0^{24h} t_{in,st}.d\tau}{24h}$$

The dampening ratio is less sensitive than error indicators to the variations of the daily mean indoor temperature, in the transient regime. So only the first 200 hours were omitted for the computation of the mean dampening ratio over the whole year.

5.4. Validation of a zone simplified model

A zone simplified model such as that presented on fig. 5.9 was built for five two levels houses and for an office room. The weather data are reference weather data recorded in Uccle, Belgium. A ventilation heat loss can be considered, based on a ventilation rate of *0.75 h⁻¹*.
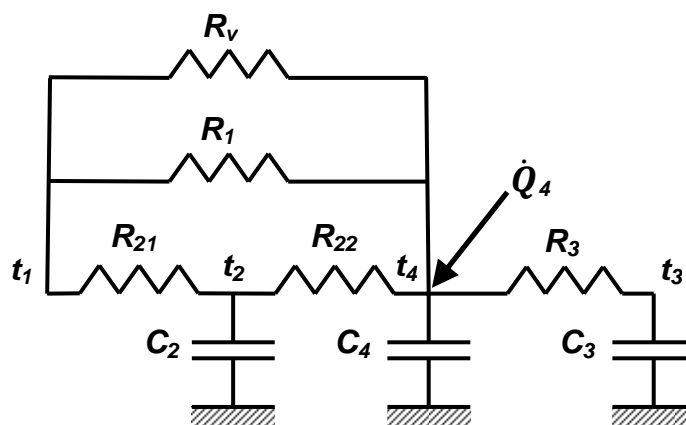

Fig. 5.9 Dynamic zone simplified model.

The parameters of the model are given in annex 4 where two types of wall parameters are involved: the *exact parameters* computed from the detailed description of the wall composition, and the *default parameters* resulting from the wall typology established in chapter 3 §3.5.

The validation process described in §5.3 can thus provide two types of results:

- A validation of the simplified model, when it is built on the *exact values* of the wall parameters ϕ θ
- A similar validation when the model is built on the *default values* of the wall parameters ϕ θ

The results provided by the model built on wall default values are less accurate than those provided by the model resulting from wall exact parameters. Anyway, if the model built on exact wall parameters can be considered as reliable, the model built on default parameters should be considered as reliable too, if the lack of accuracy is slight. This would afford a much easier way to introduce building dynamic data for the user. No need for him to describe the wall layers in detail, only four parameters being necessary: the U-value, the total heat capacity and the two non dimensional default parameters ϕ θ.

5.4.1. Daily mean temperatures and amplitudes

Those indicators give the 95% confidence intervals of the mean differences $\left(\bar{t}_{in} - \bar{t}_{in,ref} \right)$ and amplitudes differences $\left(\Delta t_{in} - \Delta t_{in,ref} \right)$ (5.7).

Fig. 5.10 represents confidence intervals related daily *mean indoor temperatures* while fig. 5.11 represents intervals associated to daily *temperature amplitudes*. Three occupancy schedules are considered: a floating temperature mode, a tertiary occupancy profile and a residential profile (fig. 5.5).
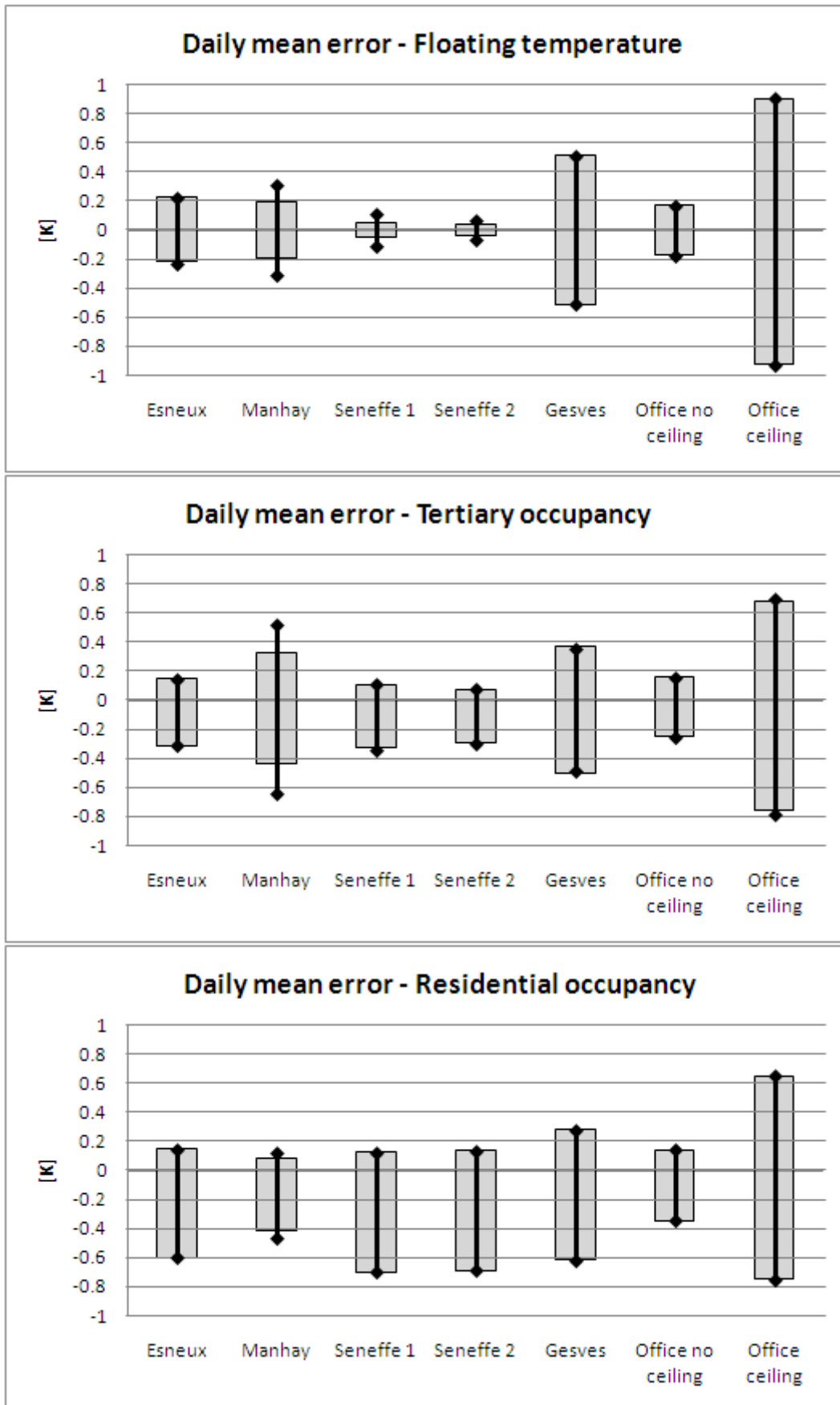
*Fig. 5.10: Confidence intervals related to the daily mean indoor temperatures.*
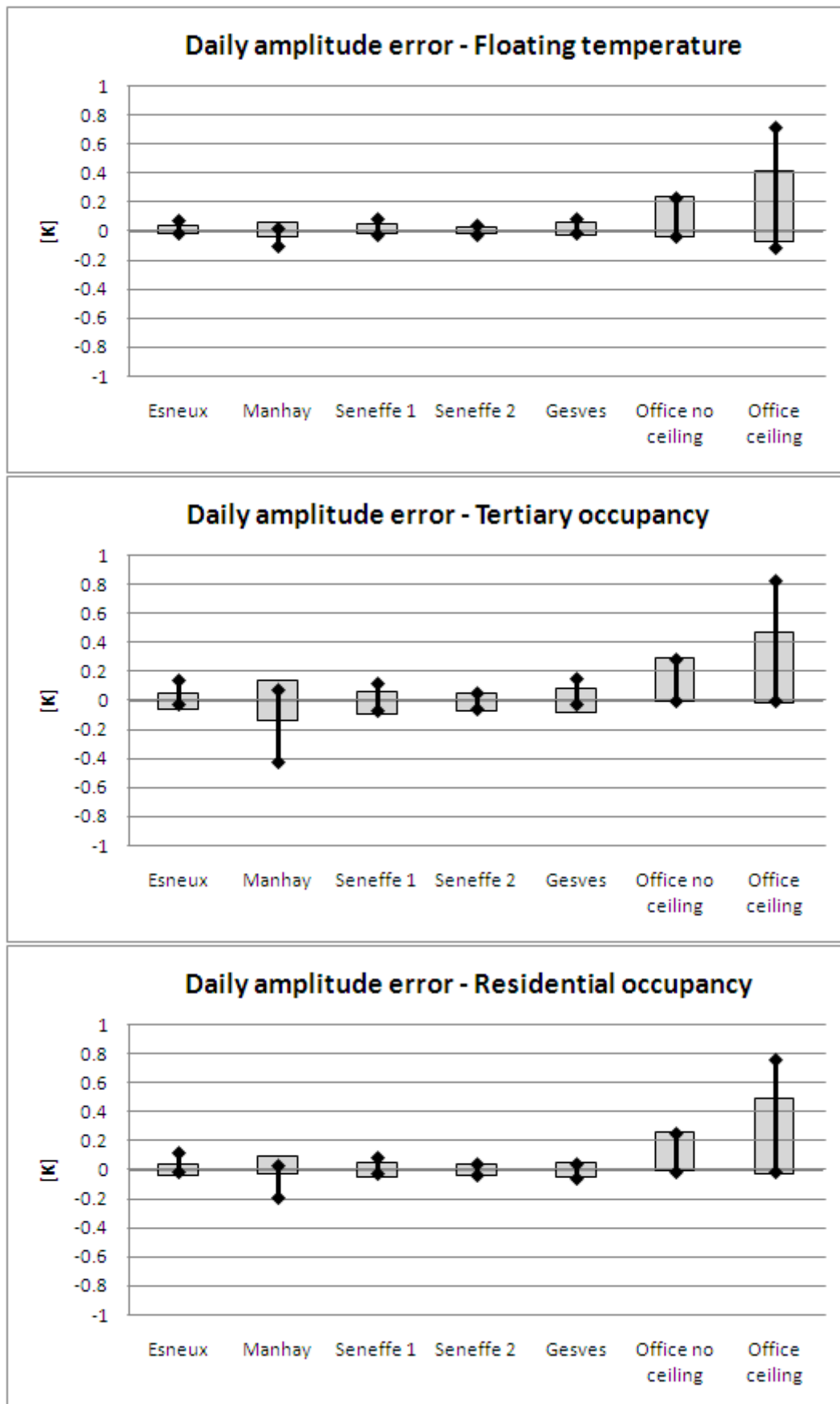
Fig. 5.11: Confidence intervals related to the daily indoor temperature amplitudes.

The confidence intervals can be computed for each house and for the office room considering both exact and default values for the walls parameters ϕ θ. Rectangles correspond to models built on walls *exact parameters*, while black lines correspond to walls *default parameters*.

The *daily means difference* remains less than *1 K,* which is acceptable. For the office room with suspended ceiling, the daily mean error is close to *1K*. A frequency analysis shows that the daily mean error reaches *1 K* for less than ten days on the year, in floating mode (fig. 5.12). So, the model can be considered as acceptable.
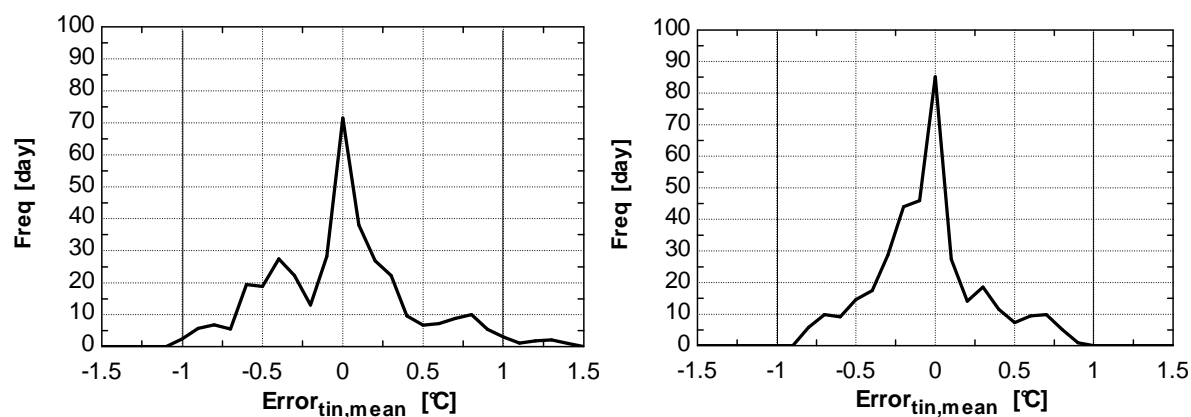
Fig. 5.12: Frequency curves of the error on the daily mean indoor temperatures, for the office room with suspended ceiling (floating temperature at left, residential occupancy at right, walls exact θ ϕ parameters for both diagrams).

The *daily amplitudes difference* remains less than *1 K*, and, again, the model can be considered as acceptable.

It should be noted that the use of ϕ θ default parameters, instead of exact parameters, to describe the wall dynamic behavior, doesn't corrupt the results too much. The higher differences can be observed for Manhay house and for the office room with suspended ceiling. In both cases, the accessibility of walls mass is low. External wall bricks are protected from the indoor space by an insulation layer for Manhay external walls. For the office room, a carpet and a suspended ceiling are insulating the floor masses from the indoor space.

5.4.2. Root mean square of the error

The third error indicator is the root-mean-square value of the difference between the reference indoor temperature and the validated indoor temperature profile, computed over the whole year (5.7). The indicator can be estimated for three occupancy schedules: a floating temperature mode, a tertiary occupancy profile and a residential profile (fig. 5.5). It is estimated for each house and for the office room, considering both exact and default values for the walls ϕ θ parameters (fig. 5.13). The indicator value increases as the occupancy profile presents more sharp variations (fig. 5.5): it is generally higher for the residential and tertiary occupancy profiles than for the floating temperature mode.

The conclusions are similar to those observed for the daily amplitude differences (§ 5.4.1) and the model can still be considered as acceptable.
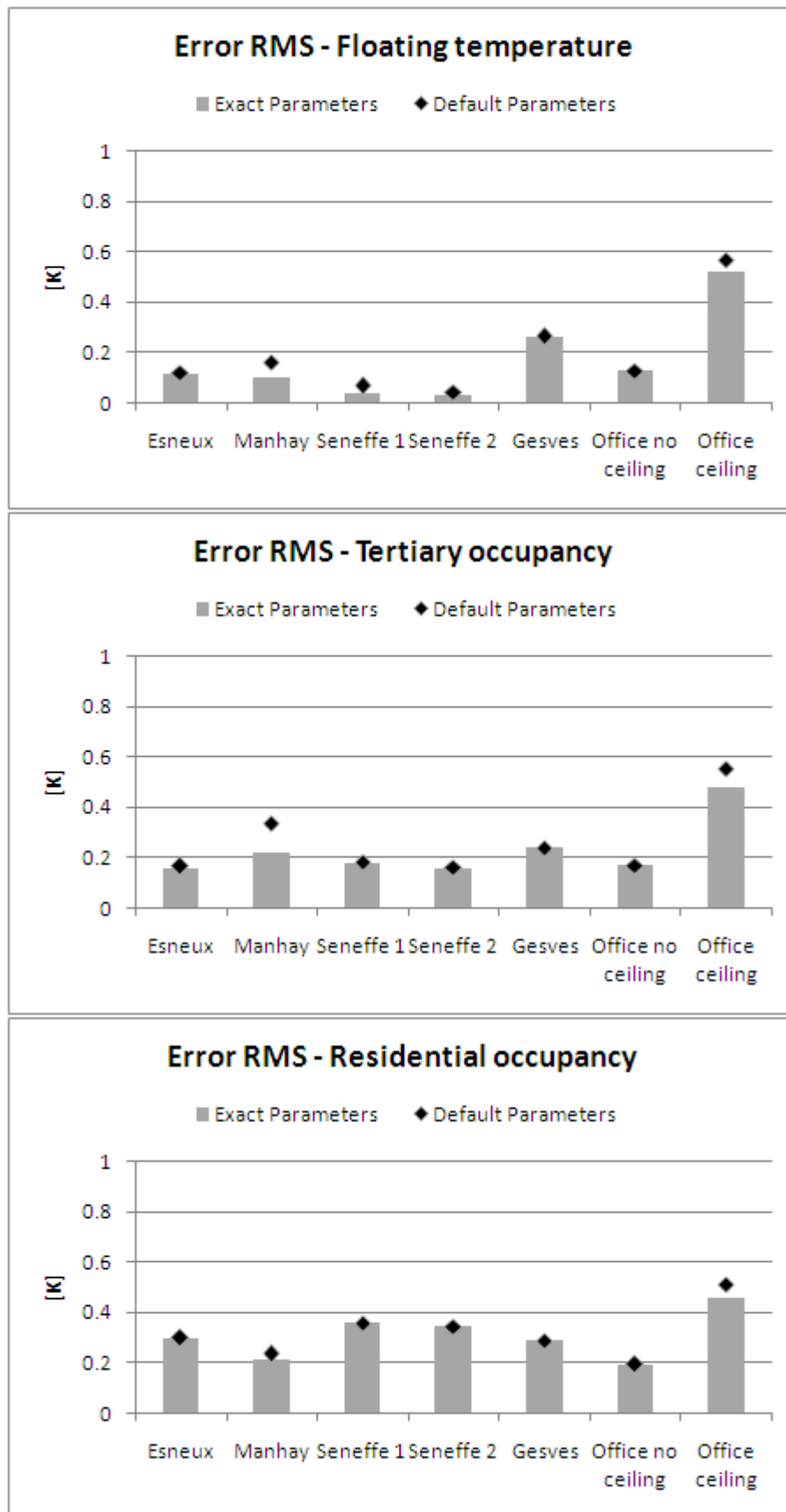
Fig. 5.13: Root-mean-square error on the indoor temperature profile over a whole year.

5.4.3. Discussion

The comparison between the detailed convolution model based on response factors, and the simplified model, could focus on the wall response factors provided by both models.

Fig 5.14 displays the response factors associated to a traditional external wall and the corresponding 2R1C network response factors. As Y response factors are small, they have a small influence on indoor temperature, while Z response factors are influencing the indoor temperature a lot.
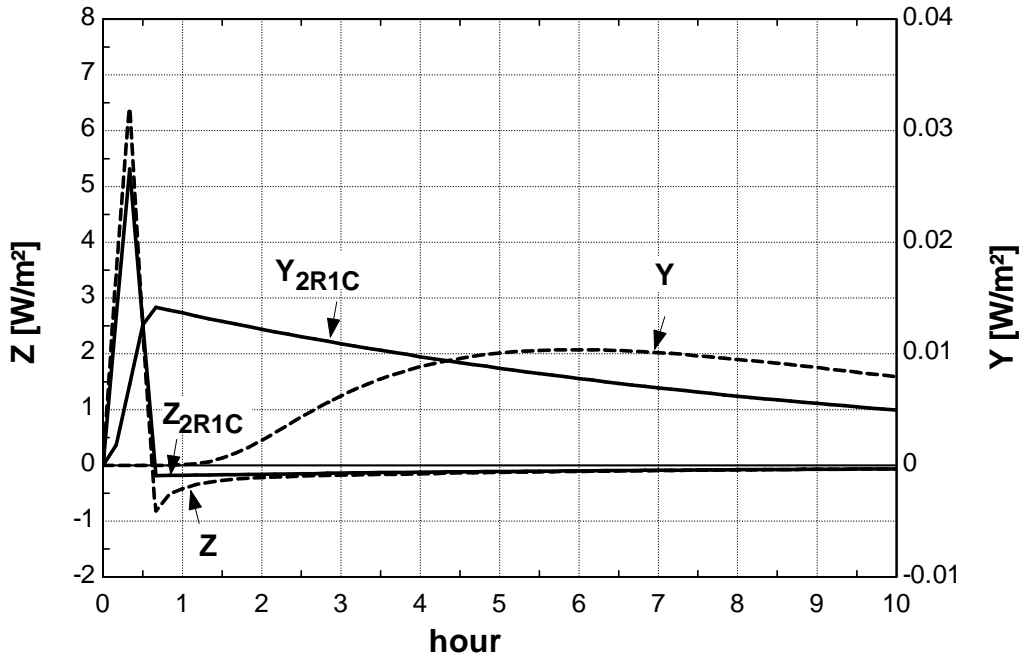
Fig.5.14. Response factors of a traditional external wall.
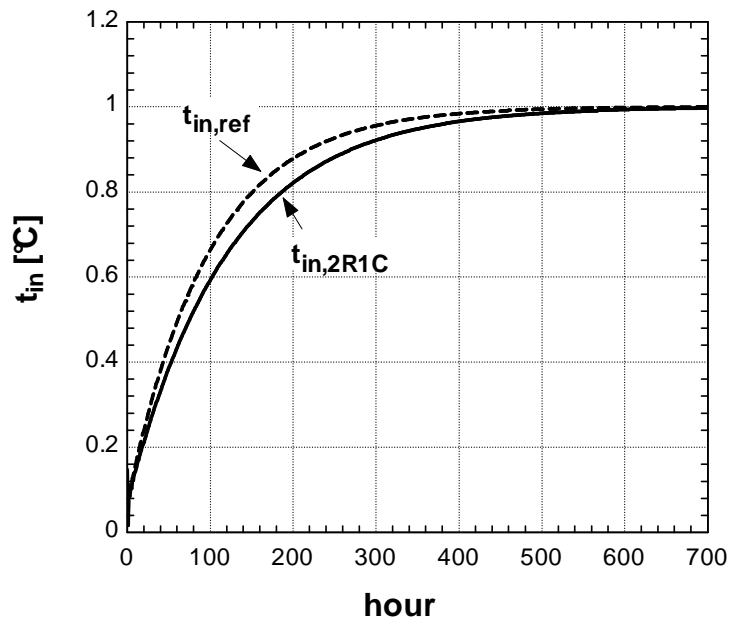
Fig.5.15. External wall response to an indoor heat flow step.

The difference between both Z curves seems to be significant, but when those response factors are integrated in a convolution process, that difference is smoothed, as can be seen on fig. 5.15 when the external wall is submitted to a step of indoor heat flow just equal to its U-value, the evolutions of the indoor temperature are close to each other for both models.

Considering the error indicators related to indoor temperature profiles in houses, maximum errors are obtained for Gesves house (fig. 5.10 and 5.11) and Manhay house (fig. 5.13). Compared to other houses, Gesves is more massive as it includes a vertical wall and a floor in contact with ground, while Manhay is lighter, including massive wooden external and internal walls instead of traditional concrete walls.
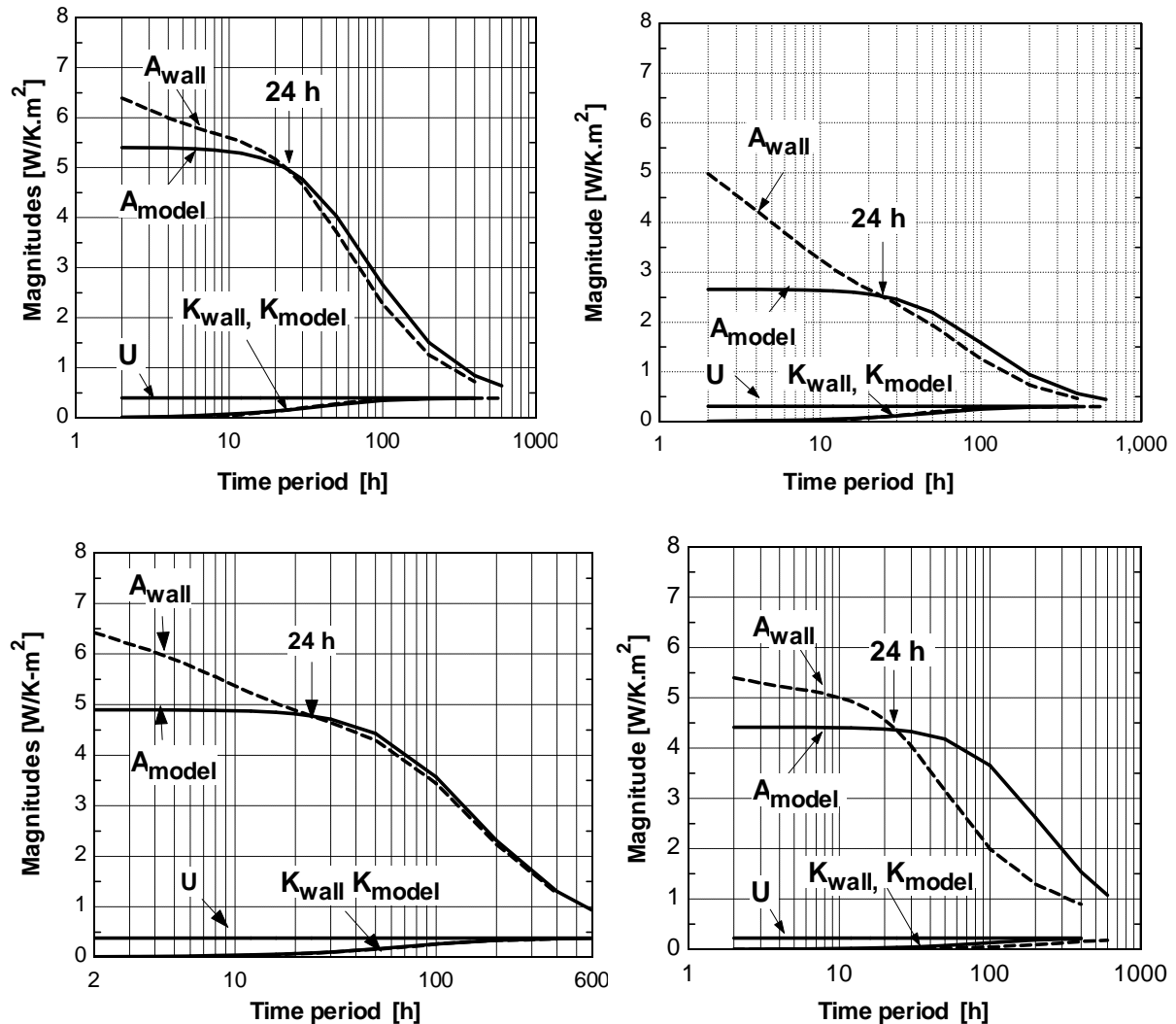
Fig.5.16. Transmittance and admittance Bode diagrams for a traditional external wall (up, left), for Manhay house external wooden wall (up, right), for Gesves house ground contact vertical walls (down, left) and ground contact floor (down, right) .

The external vertical walls Bode diagrams (fig. 5.16) show more discrepancies at high frequencies for Manhay wooden vertical walls, than for traditional concrete walls. Gesves ground contact vertical walls also show discrepancies at high frequencies, while ground contact floor presents differences for all frequencies. Those discrepancies are responsible for a lack of dampening related to indoor temperature variations, causing discrepancies in the indoor temperature profile.

Considering the error indicators related to indoor temperature profiles in offices, maximum errors are obtained for the office with suspended ceiling (fig. 5.10, 5.11 and 5.13).
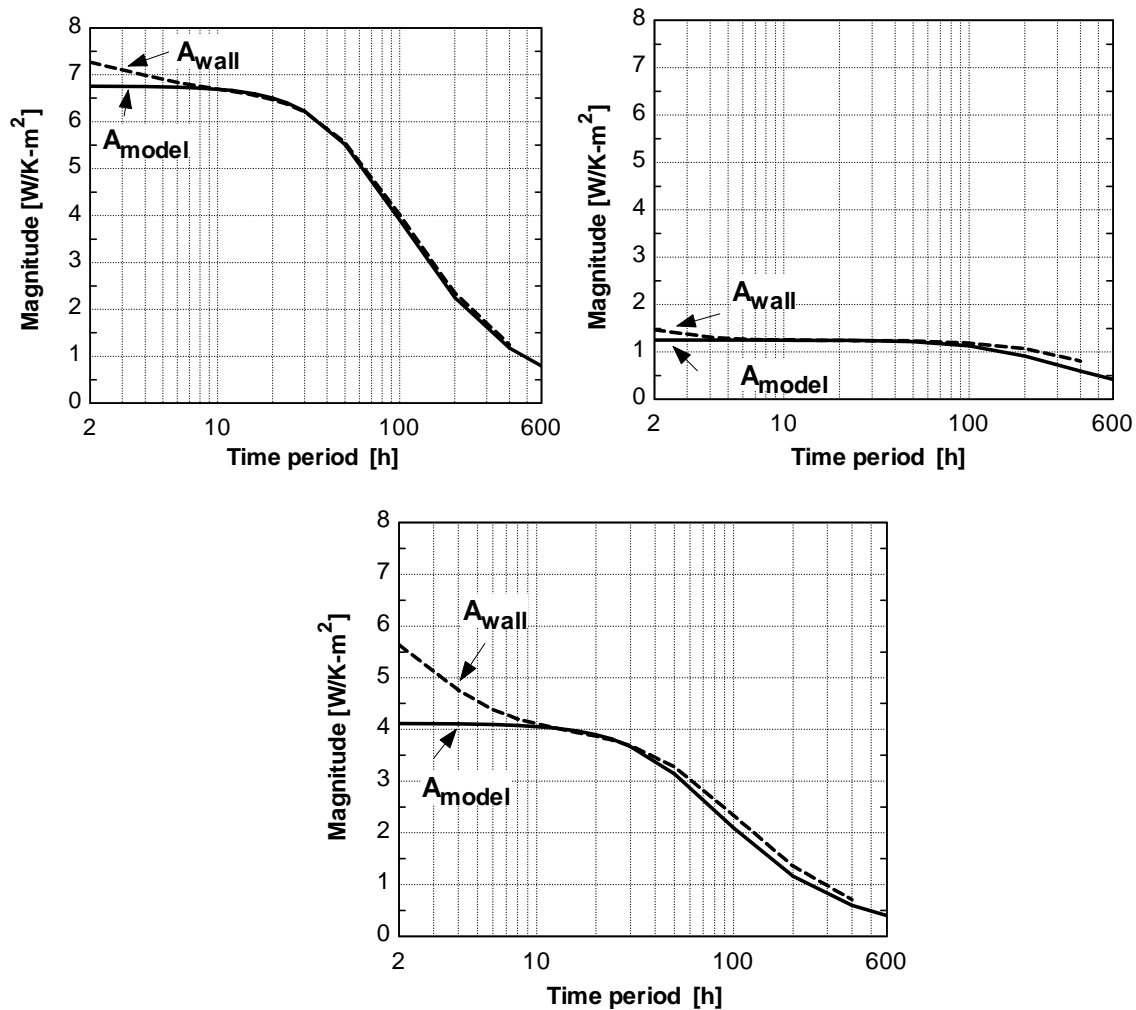
Fig.5.17. Admittance Bode diagrams for an exposed concrete ceiling (up, left), for a suspended ceiling (up, right), and for a concrete floor covered by a carpet (down).

The external vertical walls Bode diagrams (fig. 5.17) show discrepancies at high frequencies for the floor, but not so much for the ceiling, in both cases. Floor and ceiling areas are equal. For an office with exposed concrete ceiling, the global room admittance is more influenced by the ceiling admittance, as it is higher than the floor admittance, while for an office with suspended ceiling, the global admittance is more influenced by the floor whose admittance presents more discrepancies at high frequencies. So, here again, a lack of dampening related to indoor temperature variations occurs for the office room with suspended ceiling, causing discrepancies in the indoor temperature profile.

Fig. 5.18 displays the evolution of error related to the daily mean indoor temperature for both offices, in floating temperature mode. In the office room with suspended ceiling, the error increases more with indoor temperature variations, than in the office with exposed concrete ceiling.
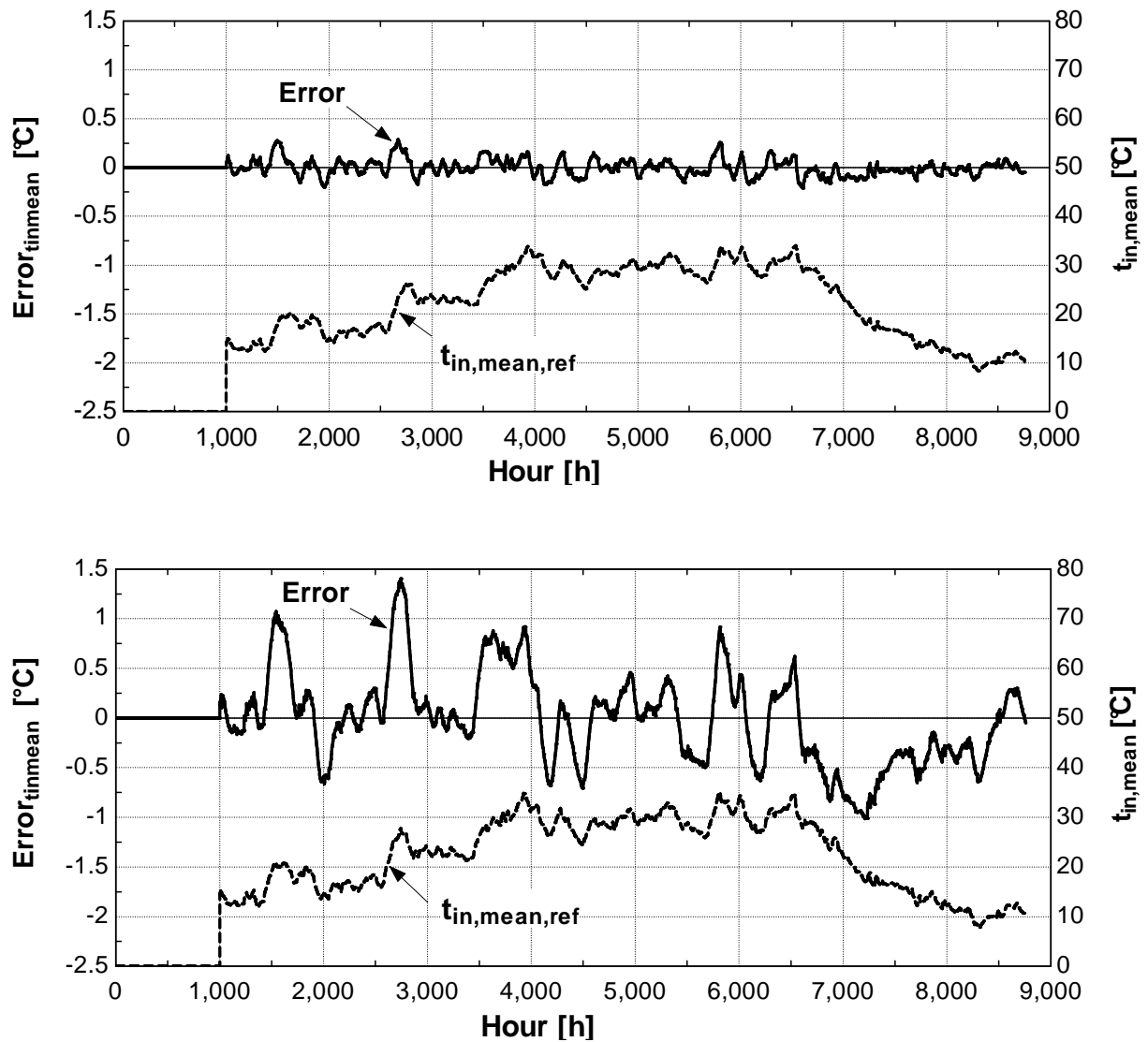
Fig. 5.18: Evolution of the error on the daily mean indoor temperature for an office room with exposed concrete ceiling (up) and for an office room with suspended ceiling (down) – floating temperature, walls exact θ ϕ parameters – Belgium reference weather data.

5.4.4. Dampening ratio

The yearly mean dampening ratio $\overline{dmp}$ accounting for the indoor temperature amplitude reduction, compared to a static computation, can characterize the building dynamic behavior (5.8).
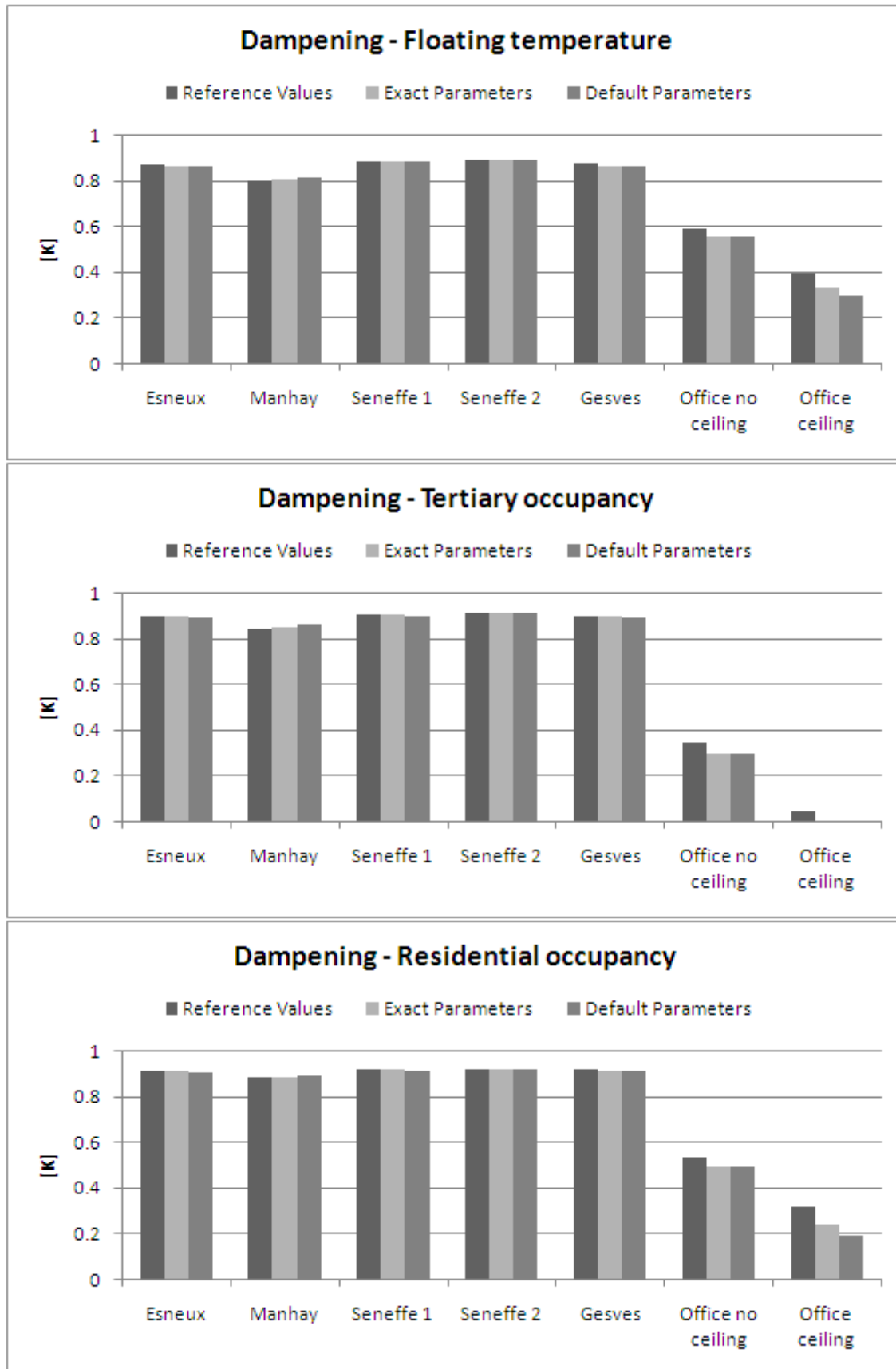
Fig. 5.19: Yearly mean amplitude dampening ratio.

The dampening is due to the building thermal mass. It can be computed for the reference indoor temperature profile as well as for the validated indoor temperature profile. In floating mode temperature, it can reach (fig. 5.19):

- 90 % for a concrete structure house
- 80 % for a massive wooden house
- 60 % for an office room with carpet and without suspended ceiling
- 40 % for an office room with carpet and suspended ceiling.

The lower values of the amplitude dampening ratio are obtained for the office room. The office building internal concrete floors are less accessible due to the presence of a carpet on the floor and/or of a suspended ceiling. The concrete structure is thus less able to store or release heat. Moreover, internal vertical walls surrounding the office room are light partitions.

A lower dampening ratio can be observed for the tertiary and residential occupancy schedules. Those patterns present several sharp variations during the day (fig. 5.5), for which the model is prompted at high frequencies. Those higher frequencies are more dampened than low frequencies whatever the model adopted (reference dynamic model based on response factors or simplified dynamic model). Bode diagrams are displayed on fig. 5.16 and 5.17: for both models, the wall admittance increases with frequency.

Now, comparing the reference and the simplified models results, for a given occupancy schedule, the simplified model response is not enough dampened for high frequencies (fig. 5.16 and 5.17), causing a lower global dampening ratio (fig. 5.19).

5.4.5. Conclusions

The results of a zone *simplified dynamic model* can be compared to those provided by a *reference* convolution model based on response factors for three types of occupancy schedules. Three error indicators can be used to compare the indoor temperature profiles generated by both models

The errors related to the daily mean indoor temperature and to the daily temperature amplitude are both lower than *1 K* most of the year, suggesting that the simplified model can be considered as reliable. The root mean square of the difference between the indoor temperatures profiles is also lower than *1 K*.

The results provided by the models built on *default values* of the walls parameters ϕ and θ are slightly different from those resulting from the model built on *exact parameters*. This implies a much easier way to introduce building dynamic data for the user. No need for him to describe the wall layers in detail, only four parameters being necessary: the U-value, the total heat capacity and the two non dimensional default parameters ϕ θ.

The yearly mean amplitude dampening ratio can be obtained by comparing the indoor temperature profiles resulting from dynamic and static computations. It ranges from 40 to 90% in floating temperature mode, depending on the wall mass and on the accessibility of that mass.

'Definition and Validation of a Simplified Multizone Dynamic Building Model Connected to Heating System and HVAC Unit'

Heating System and HVAC Unit'   *G. Masy*

5.5. Validation of a two zones simplified model

A wall model can be adopted for partition walls separating zones, so that a two zones simplified model can be generated. The model under validation is shown in fig 5.20:
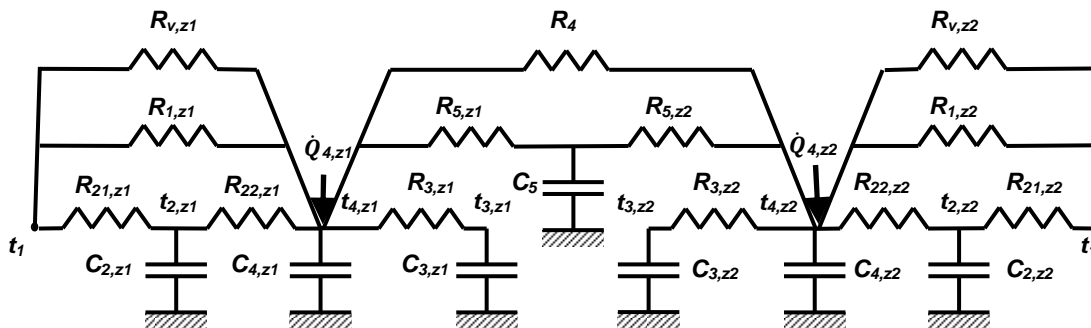

Fig. 5.20: Two zones dynamic simplified building model

A two zones simplified model is built for two of the five houses presented in chapter 4, Esneux house including concrete partition walls, and Manhay house including wooden partition walls. The partition walls related to other houses are similar to those of Esneux house.

Only the *exact parameters,* computed from the detailed description of the external and internal walls compositions, are considered.

The purpose is to validate the model proposed for partition walls which is rather rough, as mentioned in chapter 3 (§3.2.2.3). Indeed partition walls are shared by a *null heat flow plane* defined as for internal walls, and modeled through a 2R1C network, the network capacity being equal to the whole wall capacity and located at the level of the wall null heat flow plane.

Only two occupancy profiles where considered: the floating temperature mode and the residential occupancy profile. The tertiary occupancy profile wasn't considered as the daily mean errors are generally intermediate between the two others occupancy schedules (cf. §5.11). The weather data are the year reference weather data recorded in Uccle, Belgium.

5.5.1. Daily mean temperatures and amplitudes

Those indicators give the 95% confidence intervals of the mean differences $(\bar{t}_{in} - \bar{t}_{in,ref})$ and amplitudes differences $(\Delta t_{in} - \Delta t_{in,ref})$ (5.7).

The error on the daily mean indoor temperature exceeds *1 K* for a residential occupancy profile, reaching *1.1 K* which is still acceptable (fig 5.21).

The error on the daily indoor temperature amplitude is lower than *1 K*.
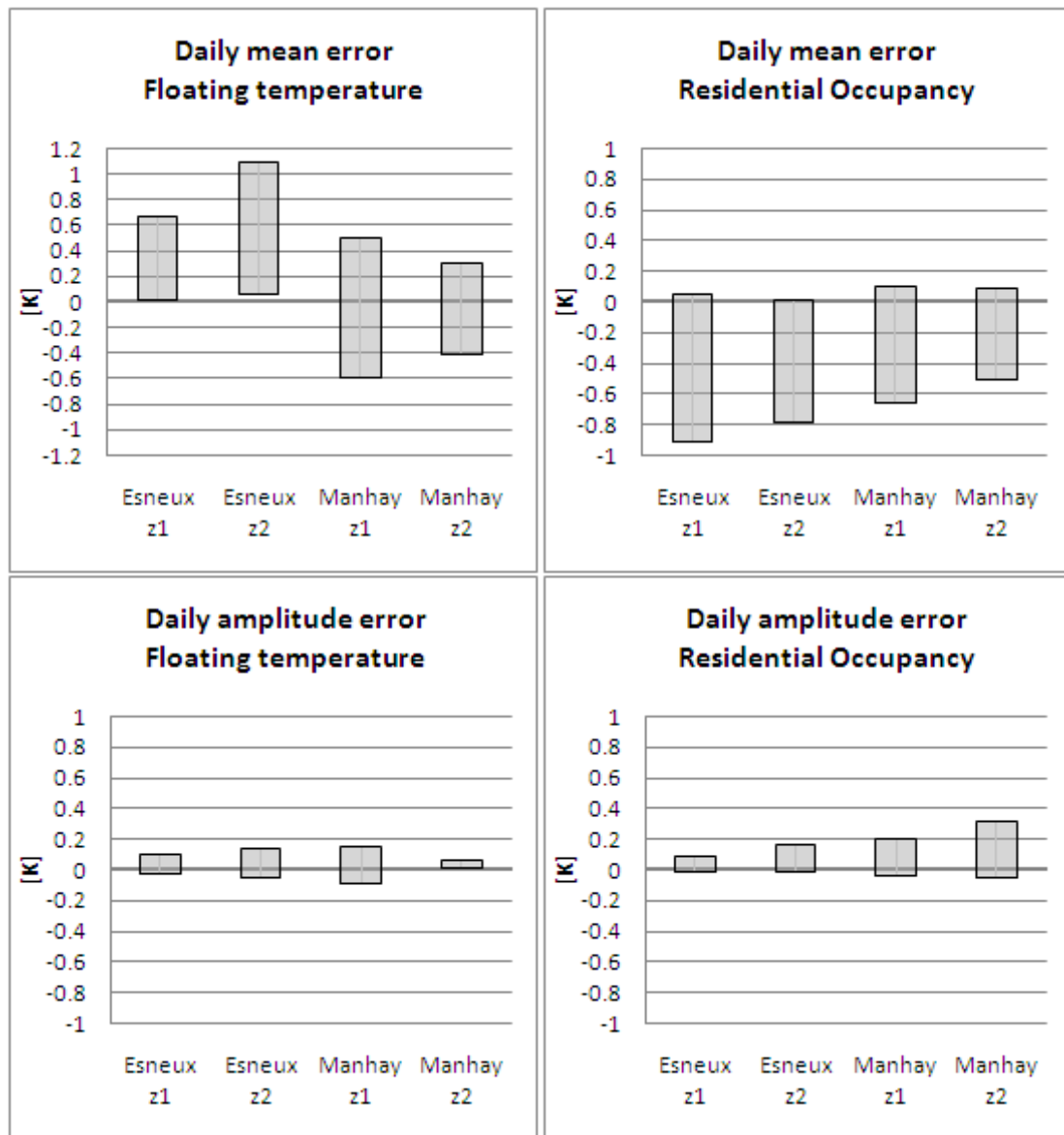
Fig. 5.21: Confidence interval of the error on the daily mean and daily amplitude related to indoor temperature, for two zones models.

5.5.2. Root mean square of the error

The third indicator is the root-mean-square value of the difference between the reference indoor temperature and the validated indoor temperature profile, computed over the whole year (5.7). It is lower than *1 K*.
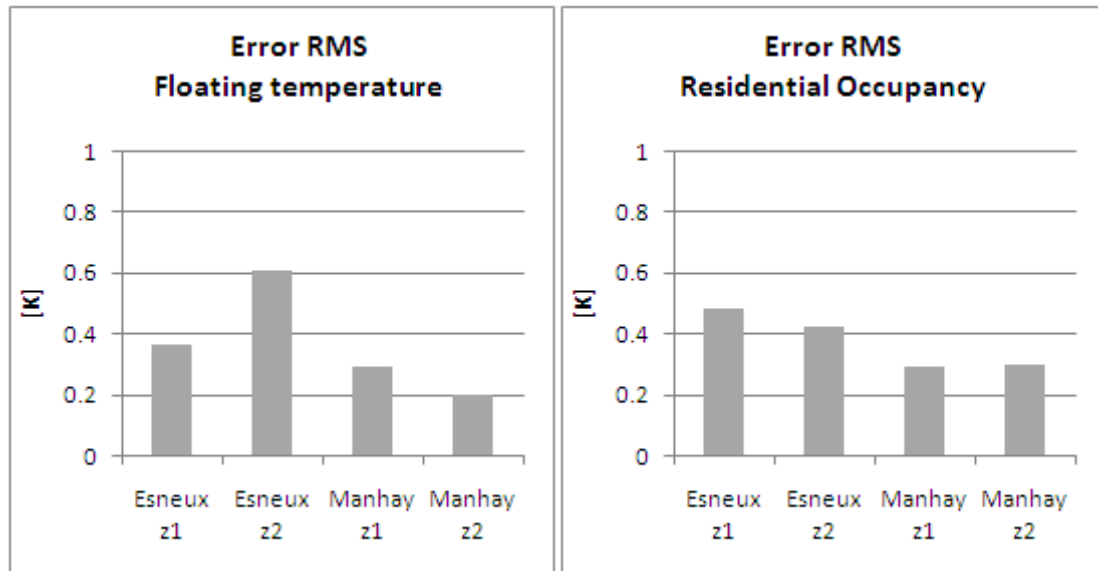
Fig. 5.22: Root-mean-square error on the indoor temperature profile computed over a whole year for two zones models.

5.5.3. Conclusions

The three error indicators related to indoor temperature profiles are lower than 1 K except for the daily mean indoor temperature associated to the floating temperature whose value slightly exceeds *1 K*. So the two zones simplified model can be considered as validated.

5.6. Solar and sky radiations

The model must be able to estimate summer overheating risks with enough accuracy. The one zone and two zones models described on fig.5.9 and 5.18 include the transmitted and absorbed solar heat gains through windows, but don't integrate the heat gains through opaque walls due to sunshine and sky radiation effects.

5.6.1. Equivalent temperature

The heat gains through opaque walls due to sunshine and sky radiation effects can be computed through an equivalent outdoor temperature defined as follows (fig. 5.23).
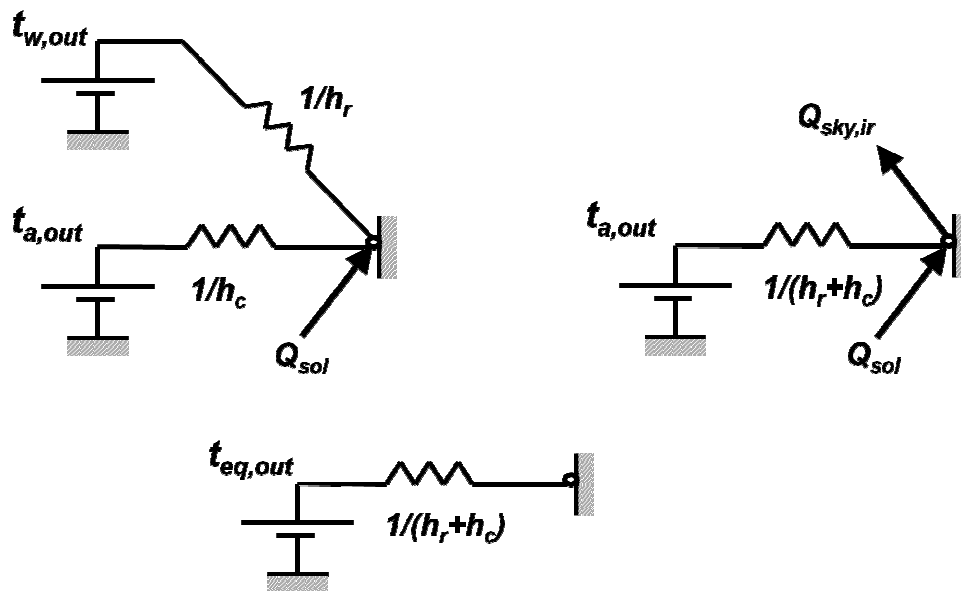
Fig. 5.23: Equivalent temperature.

The wall external surface is surrounded by the outdoor environment at temperature $t_{w,out}$ and by the air at temperature $t_{a,out}$. Heat is exchanged by radiation through a heat exchange coefficient h_r averaging *5 W/m²-K*, and by convection through a heat exchange coefficient h_c averaging *18 W/m²-K* in winter, and *12 W/m²-K* in summer.

Radiation and convection exchanges with the air temperature can be gathered through one heat exchange coefficient defined as $h_{out} = h_c + h_r$, provided a complementary radiation to the sky $\dot{Q}_{sky,ir}$ is added. That complementary radiation can be computed from equations (2.18) to (2.20), see §2.3.

Sun and sky radiations can be included in an equivalent external temperature:

$$t_{eq,out} = t_{a,out} + \frac{\alpha.\dot{Q}_{sol} - \varepsilon.\dot{Q}_{sky,ir}}{h_{out}}$$

(5.9)

α : Shortwave absorption factor - ε : Emissivity -

$t_{a,out}$: Outdoor air temperature $°C$

$\dot{Q}_{sol}$: Solar radiation reaching the wall W/m^2

$\dot{Q}_{sky,ir}$: Sky radiation W/m^2

h_{out} : Global outdoor exchange coefficient including convection and radiation transfer W/m^2K

A constant value of $h_{out} = 23$ W/m^2K can be considered for both reference and simplified models.

5.6.2. Reference model

The reference convolution model presented in (5.3) can be completed in order to account for solar and sky radiations:

(5.10)

$$\dot{Q}_{14,li,out,iso} = \sum_{i=1}^{n-1} Y_{i.\Delta t} . t_{out,t-(i-1).\Delta t} + Y_{n\Delta t} . \sum_{j=1}^{j\max} \lambda_{li,out,iso}^{j} . t_{out,t-(n+j)\Delta t} +$$

$$\sum_{i=1}^{n-1} Y_{roof,i.\Delta t} . \left(t_{eq,roof,t-(i-1).\Delta t} - t_{out,t-(i-1).\Delta t} \right) + Y_{roof,n\Delta t} . \sum_{j=1}^{j\max} \lambda_{li,roof}^{j} . \left(t_{eq,roof,t-(n+j)\Delta t} - t_{out,t-(n+j)\Delta t} \right) +$$

$$\sum_{i=1}^{n-1} Y_{wallsout,i.\Delta t} . \left(t_{eq,wallsout,t-(i-1).\Delta t} - t_{out,t-(i-1).\Delta t} \right) + Y_{wallsout,n\Delta t} . \sum_{j=1}^{j\max} \lambda_{li,wallsout}^{j} . \left(t_{eq,wallsout,t-(n+j)\Delta t} - t_{out,t-(n+j)\Delta t} \right)$$

$$\lambda_{li,roof} = \frac{AU_{roof} - \sum_{i=1}^{n} .Y_{roof,i\Delta t}}{AU_{roof} - \sum_{i=1}^{n} .Y_{roof,i\Delta t} + Y_{roof,n\Delta t}} \qquad \lambda_{li,wallsout} = \frac{AU_{wallsout} - \sum_{i=1}^{n} .Z_{wallsout,i\Delta t}}{AU_{wallsout} - \sum_{i=1}^{n} .Z_{wallsout,i\Delta t} + Z_{wallsout,n\Delta t}}$$

$\dot{Q}_{14,li,out,iso}$: Indoor heat flow response to the outdoor equivalent temperature W

5.6.3. Simplified model
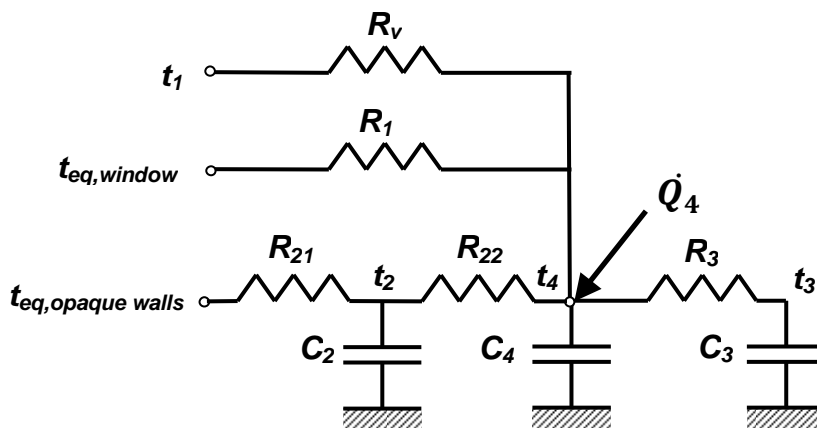
Fig. 5.24: Simplified model of one building zone including equivalent temperatures.

The simplified model defined on fig. 5.7 can also be completed in order to consider solar and sky radiations. In a first approach, an equivalent temperature is applied to the opaque external walls node in order to account for absorbed solar gains and infrared losses (fig. 5.24) and an equivalent temperature is applied to windows in order to account for sky radiation.

The model of Esneux house can be submitted to a floating mode temperature. The maximum difference between the reference and the validated indoor temperature profile is 0.43 K. So the model can be adopted but it requires a description of the opaque wall areas for each orientation, from the user.

In order to make the data introduction process easier, only solar and sky radiation related to the roof can be considered, solar and sky radiation related to vertical walls being neglected. Indeed, their impact is small compared to the roof one: because of its horizontal or nearly horizontal position, the sky proportion viewed by a roof is about two times that viewed by a vertical wall.

A first method was tested to improve the model described on fig. 5.24, by treating the light roof as purely resistive and gathered with windows and doors in the same external branch, which is provided with an equivalent outdoor temperature. Comparisons were performed with a detailed model such as TRNSYS for the fourth house (Gesves) (ref. [8]). The indoor temperature profile yield by the model is close to the profile yield by TRNSYS. Anyway, it was decided to separate the roof resistance from the window one, and to provide it with its own capacity because even if light roofs and windows are close to each other as far as capacity is concerned, their time constants are quite different:

Double window 2x5mm: C = 21000 J/K.m² $\tau =$ 1,6 h
Wooden structure roof: C = 20000 J/K.m² $\tau = 14,6$ h
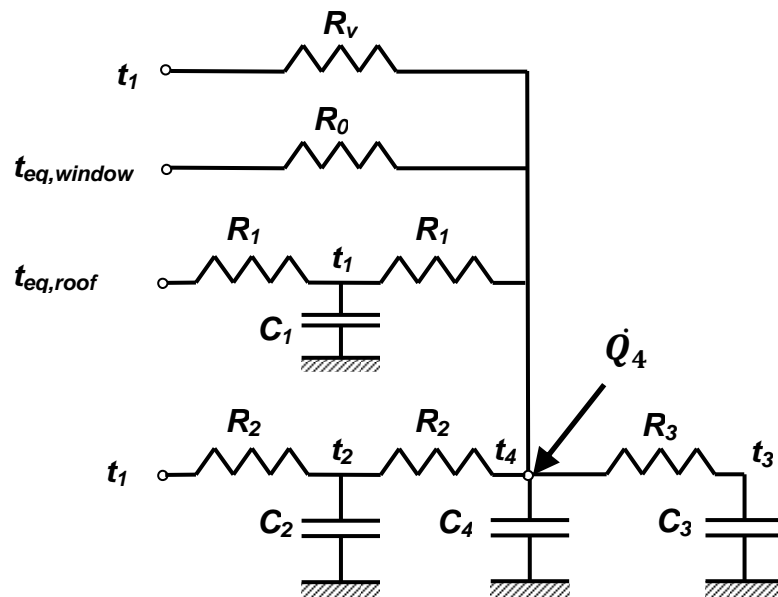
Fig. 5.25: Simplified model of one building zone including specific branches provided with different equivalent outdoor temperatures.

So, in a second approach, the simplified model is replaced by a four external branches model (fig. 5.25):

- The first branch is accounting for ventilation exchanges. It is connected to outdoor temperature.
- The second branch is purely resistive accounting for light walls such as windows and doors. It is connected to an equivalent temperature involving the sky radiation effect.
- The third branch is provided with a capacity to model the roof which can be either light or massive. It is connected to a specific equivalent temperature involving the solar and sky radiation effects.
- The fourth branch is provided with a capacity to model other massive external walls. It is connected to outdoor temperature.

The results provided by this model can be compared to those computed through a detailed model based on a convolution process (5.10). The detailed model includes all the sunshine and sky radiations, i.e. related to all external opaque walls orientations including vertical walls. The comparison can be performed for the five two levels houses presented in annex 2. The weather data are those measured during the 1976 summer hot wave. The initial indoor and outdoor temperatures are equal to 25°C for both models. The first 24 h results can be removed for the computation of error indicators.

Fig. 5.26 displays the computed indoor temperatures profiles for Manhay house. Fig. 5.27 shows the values of error indicators (5.7). Rectangles correspond to models built on walls *exact parameters*, while black lines correspond to walls *default parameters*.
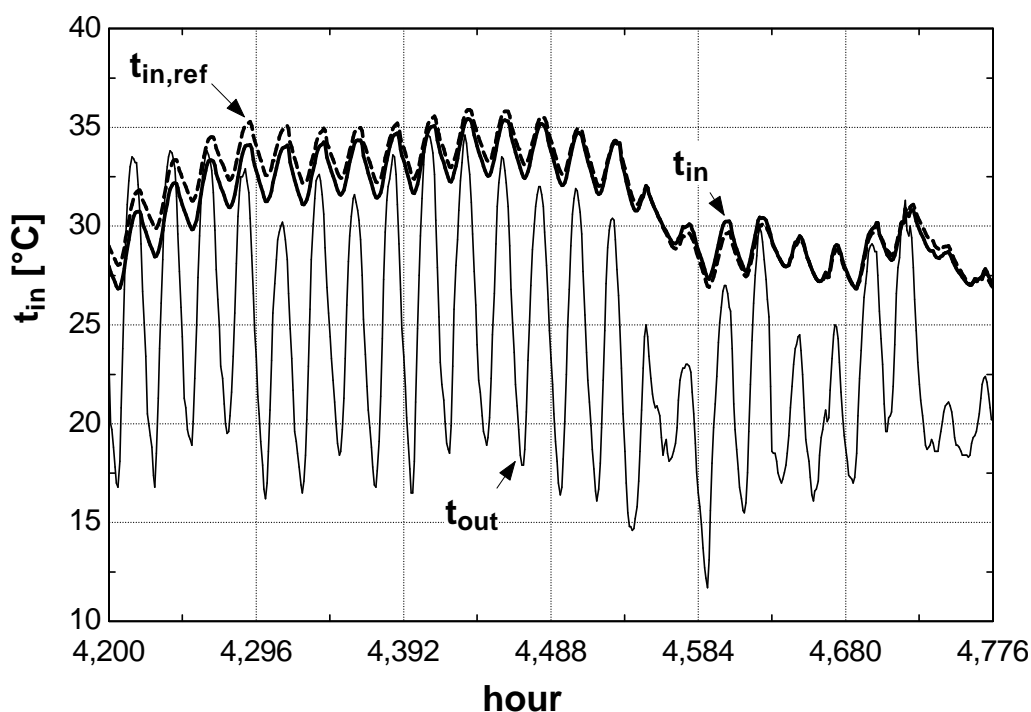

Fig. 5.26. Indoor temperatures provided by the simplified dynamic model of fig 5.25, and by a detailed model, for Manhay house, during 1976 hot wave.
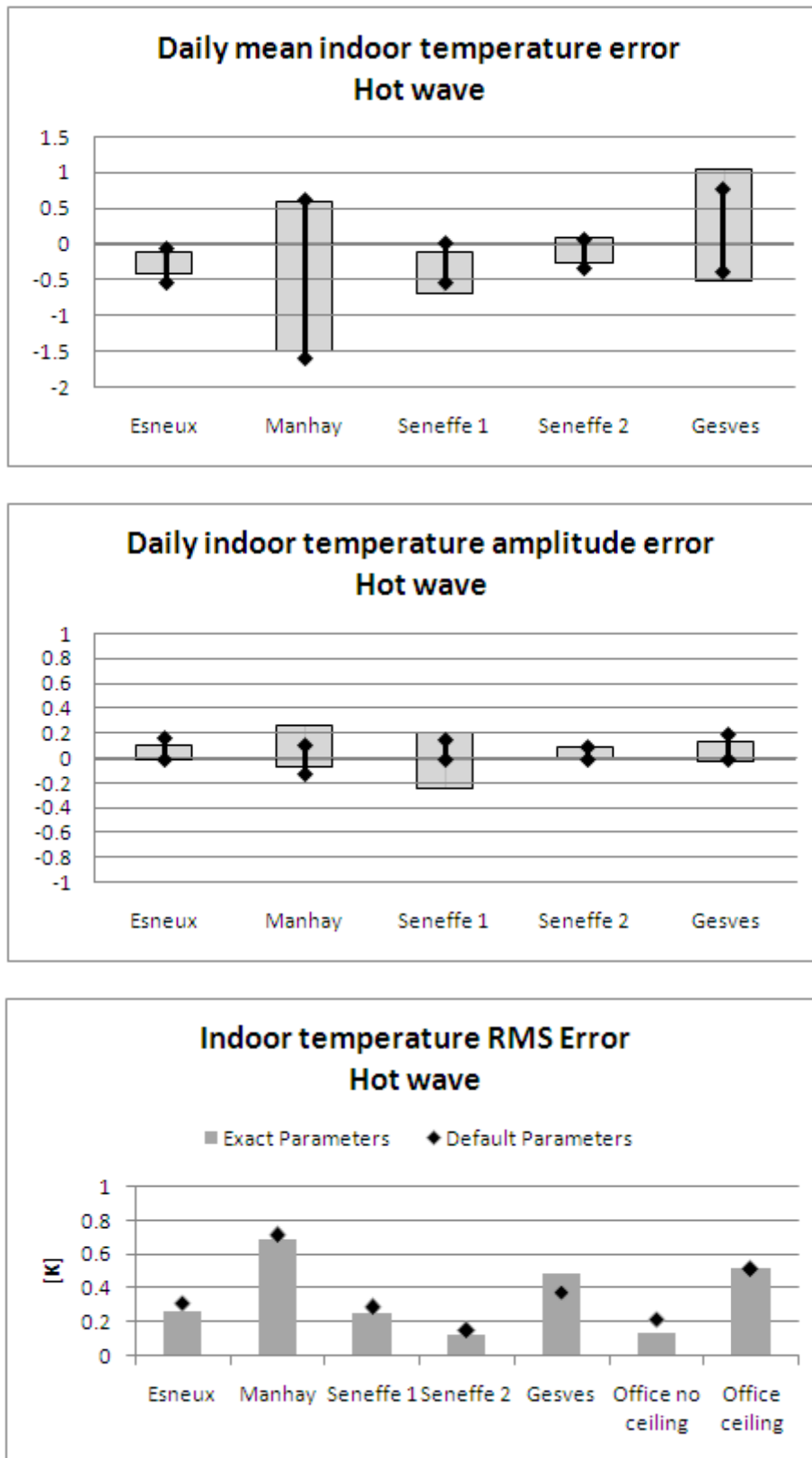
Fig. 5.27: Error indicators computed for 5 houses over 1976 summer hot wave.

The daily mean temperature difference exceeds *1K* for Manhay house (fig. 5.27). Anyway the *-1.5 K* value is overestimated because the frequency distribution of the error is not Gaussian. In fact, a minimum value of *-1.3 K* is observed at the beginning of the error evolution (fig. 5.28, up). That value can be partially explained by the differences related to sun and sky radiations on opaque walls. Indeed, the simplified model only accounts for those radiations on the roof, while the reference model includes radiations on all the external opaque walls. The error reaches *-1.08 K* when both models are only accounting for radiations on the roof (fig. 5.28, down).

Compared to other houses, Manhay includes massive wooden vertical walls protected by an insulation layer and a brick. Those vertical walls are lighter than traditional concrete ones and seem to be more sensible to solar radiation, which is neglected in the simplified model.
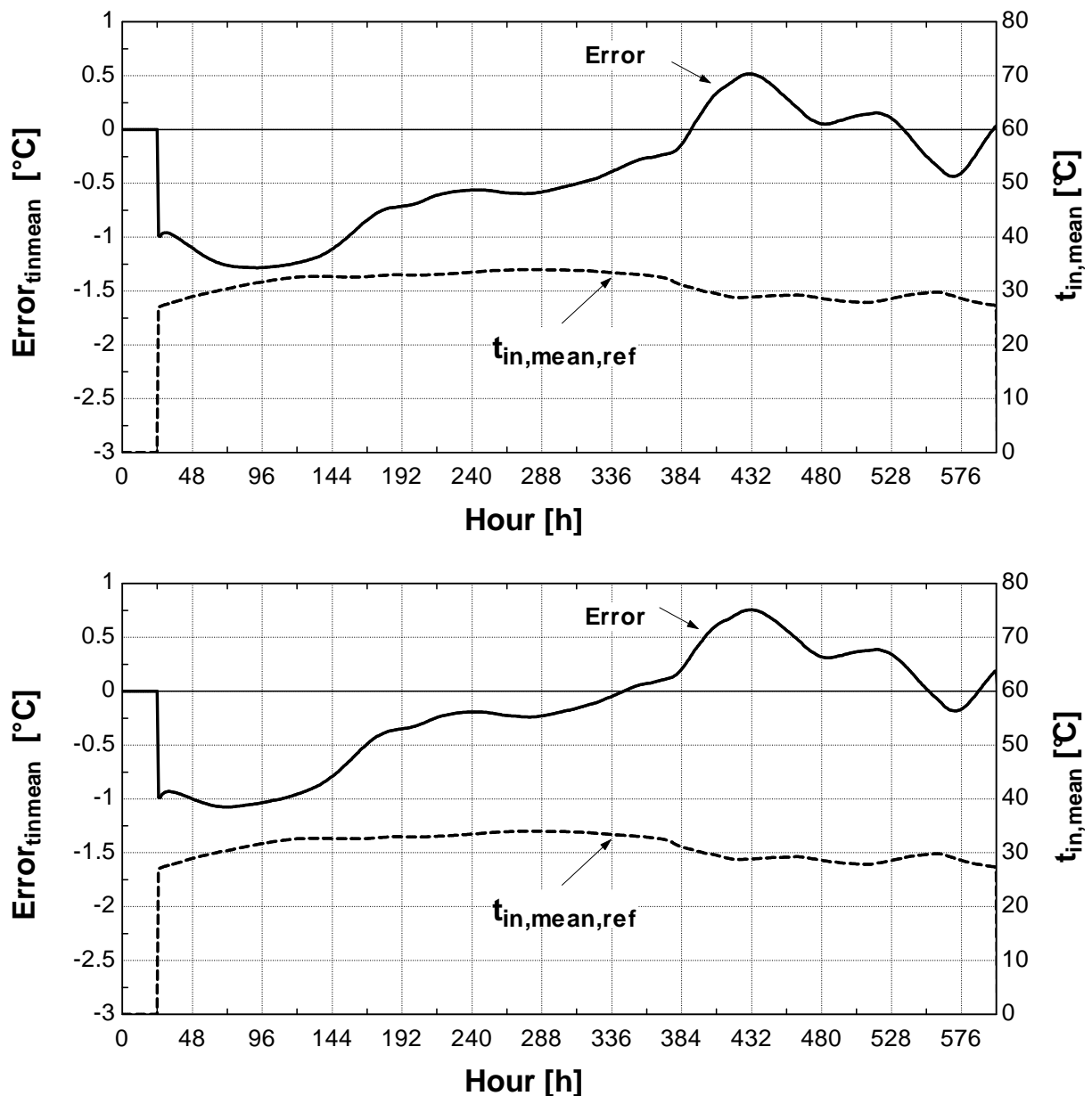

Fig. 5.28: Evolution of the error on the daily mean indoor temperature for Manhay house submitted to 1976 hot wave: the reference model includes sun and sky radiations on all the external walls (up) or on the roof only (down).

The evolution of the error also suggests that the model is prompted in transient regime. Such a regime normally appears with a hot wave, but its effects might be exaggerated as the initial indoor temperature seems to be underestimated: it should average 28 °C instead of 25°C.

Other error indicators are lower than *1K*. So the model can be considered as validated.

5.6.4. Conclusions

The resulting simplified model can be compared to a detailed response factors convolution model including solar and sky radiation related to all the opaque walls. In order to avoid a description of the opaque wall areas for each orientation, it was decided to only consider absorbed solar gains and infrared losses related to the roof and to neglect absorbed solar gains and infrared losses related to vertical walls.

The simplified model is thus considered as reliable. The floating indoor temperature profiles occurring during a hot wave can be compared for five houses through several error indicators. All of them are lower than *1K*, except for the daily mean indoor temperature associated to Manhay house whose value reaches *1.3 K*.

5.7. Experimental validation

The model can be tested on the experimental results provided by EMPA test cell (fig. 5.29) in the framework of IEA-ECBCS annex 43 research project (ref. [40]). The cell is composed of tight insulated steel sandwich boards and the window is removed. The thermal characteristics are well known, disturbances caused by the occupants as well as solar and sky radiations are not present.
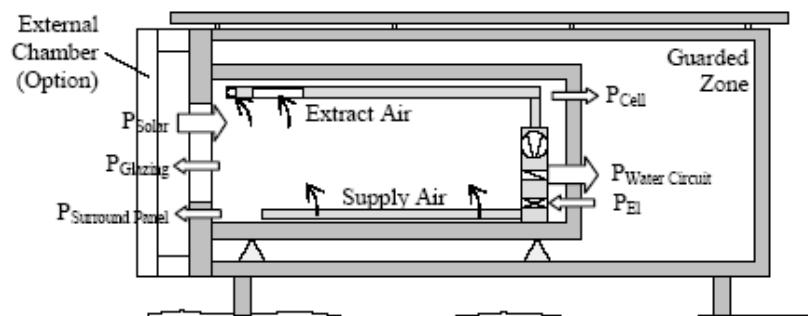

*Fig 5.29 : EMPA test cell (2.36 m x 2.85 m x 4.63 m)*
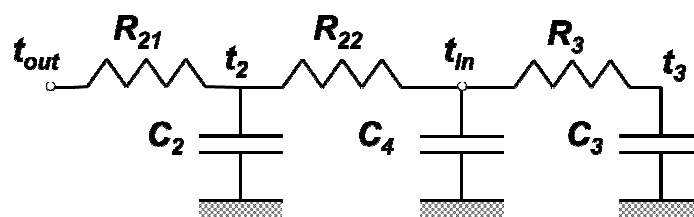
Fig 5.30 Zone simplified model of the EMPA test cell.

A zone simplified model (Fig. 5.30) can be generated from the exact description of the walls compositions, with the following characteristics, C_3 representing the furniture heat capacity:

$R_{21}= 0.05591$ K/W $\qquad$ $R_{22}= 0.01386$ K/W $\qquad$ $R_3 = 0.000625$ K/W
$C_2 = 503284$ J/K $\qquad$ $C_3 = 200000$ J/K $\qquad$ $C_4 = 189942$ J/K

The environment can be controlled so that outdoor temperature is known. Air heating system flows are given (fig. 5.31), as well as corresponding indoor temperatures.
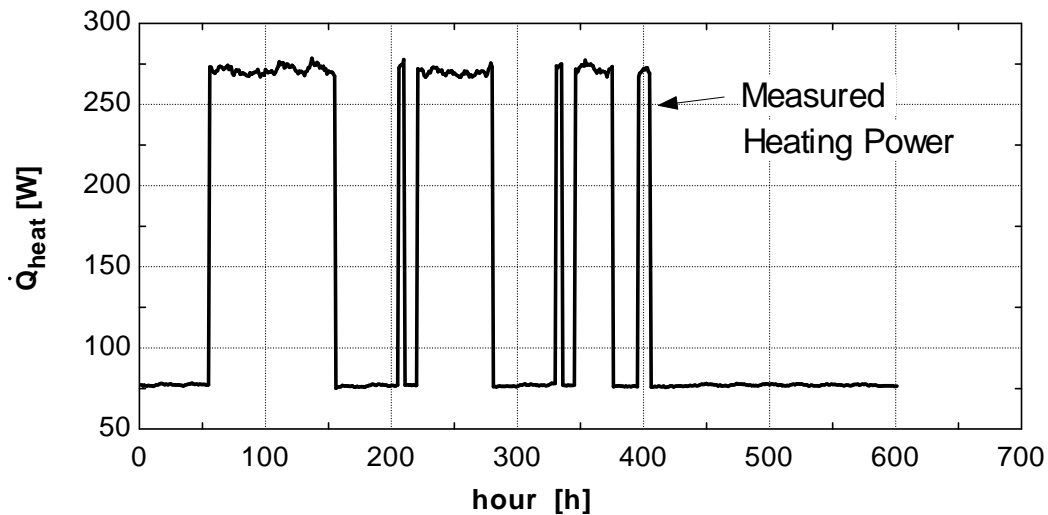

Fig 5.31 Comparison of measured (dotted line) and computed (full line) indoor temperatures

The indoor temperatures computed by the model for imposed heat flows can be compared to measured indoor temperatures (Fig. 5.32). The RMS of the error related to indoor temperature equals 0.46 *K*.
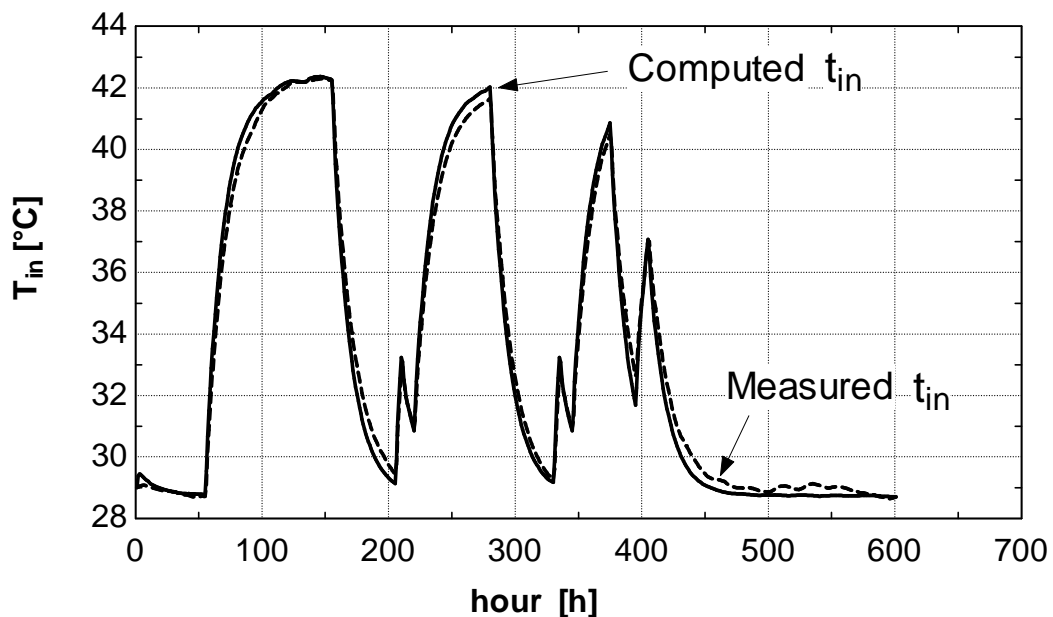

Fig 5.32 Comparison of measured (dotted line) and computed (full line) indoor temperatures

The quality of the results provided by the model in this validation test can be underlined, as the EMPA test cell is here submitted to rather unrealistic step sollicitations, while the simplified model is built on wall responses to sinusoidal sollicitations for a 24h time period.

5.8. Conclusion

The results of the *simplified dynamic model* proposed in §4.3 and 4.4 can be compared to those provided by a *reference* convolution model based on response factors [24], [25]. The comparison can be performed over a whole year computation with a 20 min time step, for a set of representative houses and for an office room.

Three error indicators can be used to compare the indoor temperature profiles generated by both models (§5.3). The dampening factors can also be computed by comparison with a simple static model.

The error on the daily mean indoor temperature as well as on the daily temperature amplitude are both lower than *1 K* suggesting that a zone simplified model can be considered as reliable. The root mean square of the difference between the indoor temperatures profiles is lower than *1 K* also.

For the two zone model, the errors related to the indoor temperature profile are generally higher than those observed for the one zone model, probably because the model of the *partition* wall is rather rough. Anyway, the error doesn't exceed significantly *1 K*.

The results provided by the models built on *default values* for the wall parameters ϕ and θ are slightly different from those resulting from the model built on *exact parameters*. This implies a much easier way to introduce building dynamic data for the user. No need for him to describe the wall layers in detail, only four parameters being necessary: the U-value, the total heat capacity and the two non dimensional default parameters ϕ θ.

The yearly mean amplitude dampening ratio obtained by comparing the indoor temperature profile resulting from dynamic computation, and a static computation profile, reaches:

- 90 % for a concrete structure house
- 85 % for a massive wooden house
- 55 % for an office room with carpet and without suspended ceiling
- From 5 to 40 % for an office room with carpet and suspended ceiling.

In order to avoid a description of the opaque wall areas for each orientation, only solar and sky radiations related to the roof can be considered in the simplified model, solar and sky radiation related to vertical walls being neglected. The resulting simplified model can be compared to a detailed response factors convolution model solar and sky radiation on all external opaque walls. The floating indoor temperature profiles occurring during a hot wave can be compared for five houses. Error indicators are lower than *1K*, except for the daily mean indoor temperature associated to Manhay house whose value reaches *1.3 K*.

The one zone simplified dynamic model was tested on experimental results provided by a test cell composed of tight insulated steel sandwich boards. The RMS of the error related to indoor temperature equals *0.46 K*. The quality of the results provided by the model in this validation test can be underlined, as the test cell was submitted to rather unrealistic step sollicitations, while the simplified model is built on wall responses to sinusoidal sollicitations for a 24h time period.

In conclusion, the simplified model is considered as reliable.

Two simplified models can be implemented in the framework of SISAL research project, supported by 'Région Wallonne' [49], [50].

From the network of fig. 5.25, a two zone R-C network can be built in order to perform simulation on houses. Both zones RC networks can be connected to each other through a set of resistances and capacities (fig. 5.33):

- Resistance R_4 models the effect of light walls such as doors.

- Resistances $R_{5,z1}$, $R_{5,z2}$ and capacity C_5 represents the massive partition walls interconnecting the two zones.
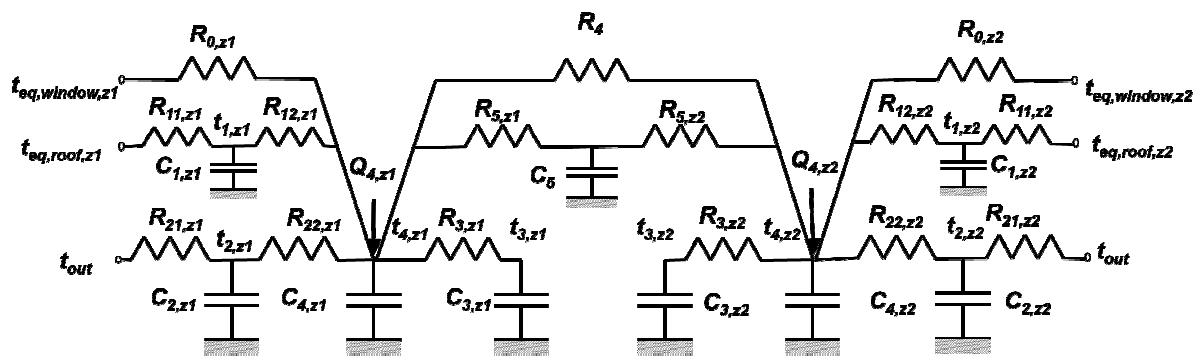

Fig. 5.33: Two zones dynamic simplified building model

The ventilation exchanges are not represented on this model as they will be dealt with in chapter 6.

The first zone can be the ground floor of a two storey house, and the second zone can be a first floor occupied during the night. The first zone could also represent a house central zone completely surrounded by a zone of heated rooms at the same level. Simulation on such a model could help to answer the question: is it necessary to heat the central room to reach its indoor temperature set point?

From the network of fig. 5.25, again, a five zones R-C network can be built for *office buildings*. Offices are submitted to similar indoor temperature profiles, so that the partition walls separating them can be shared in two parts, both submitted to adiabatic boundary conditions.

Four resulting RC networks are then connected to each other through a set of resistances and capacities (fig. 5.34):

- Resistance R_4 models the effect of light walls, such as doors between each office and the corridor

- Resistances R_5 and capacity C_5 represents the massive partition walls connecting each office to the corridor.

Here again, the ventilation exchanges are not represented as they will be dealt with in chapter 6.
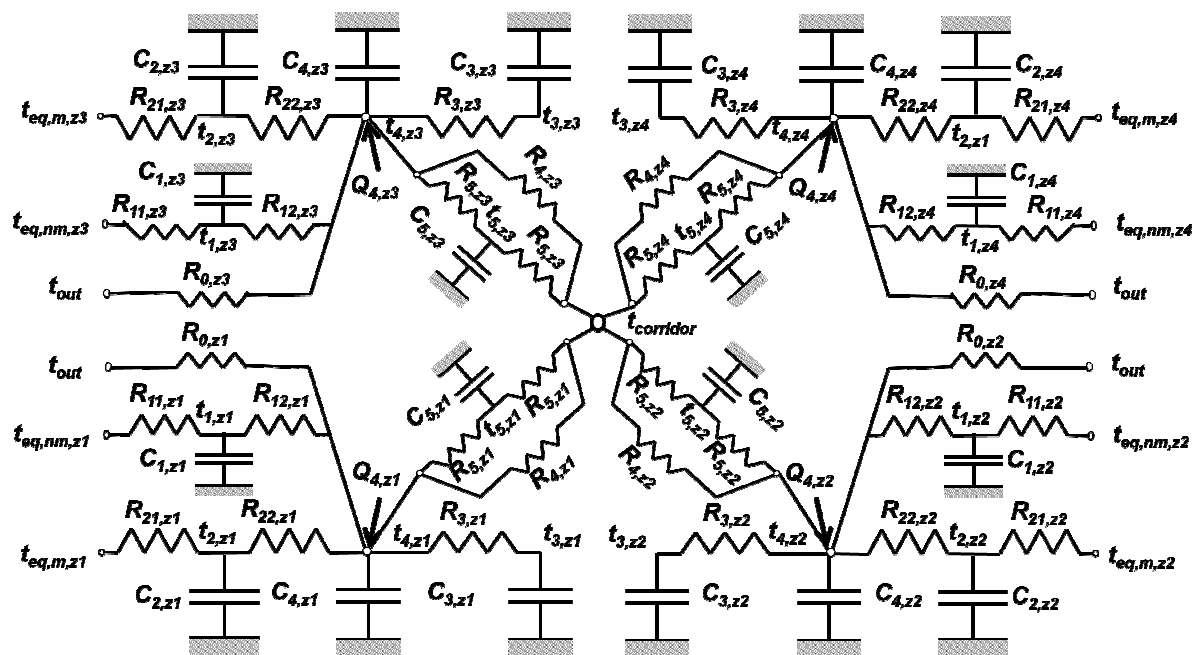
Fig. 5.34. Four zones dynamic simplified office building model

Such a model can handle four offices with various external windows areas and with different orientations. Combined with a five zones ventilation model (see chapter 6), it can be used to perform air quality analysis (see chapter 7) or thermal comfort studies (see chapter 8).